



Measurement of the total cross section from elastic scattering in pp collisions at $\sqrt{s} = 8$ TeV with the ATLAS detector

著者	The ATLAS Collaboration , Hara K., Kim S.H., Okawa H., Sato K., Ukegawa F.
journal or publication title	Physics letters. B
volume	761
page range	158-178
year	2016-10
権利	(C) 2016 The Author. Published by Elsevier B.V. This is an open access article under the CC BY license (http://creativecommons.org/licenses/by/4.0/). Funded by SCOAP 3 .
URL	http://hdl.handle.net/2241/00145334

doi: 10.1016/j.physletb.2016.08.020



Measurement of the total cross section from elastic scattering in pp collisions at $\sqrt{s} = 8$ TeV with the ATLAS detector



The ATLAS Collaboration*

ARTICLE INFO

Article history:

Received 25 July 2016

Received in revised form 9 August 2016

Accepted 9 August 2016

Available online 16 August 2016

Editor: W.-D. Schlatter

ABSTRACT

A measurement of the total pp cross section at the LHC at $\sqrt{s} = 8$ TeV is presented. An integrated luminosity of $500 \mu\text{b}^{-1}$ was accumulated in a special run with high- β^* beam optics to measure the differential elastic cross section as a function of the Mandelstam momentum transfer variable t . The measurement is performed with the ALFA sub-detector of ATLAS. Using a fit to the differential elastic cross section in the $-t$ range from 0.014 GeV^2 to 0.1 GeV^2 to extrapolate $t \rightarrow 0$, the total cross section, $\sigma_{\text{tot}}(pp \rightarrow X)$, is measured via the optical theorem to be

$$\sigma_{\text{tot}}(pp \rightarrow X) = 96.07 \pm 0.18 \text{ (stat.)} \pm 0.85 \text{ (exp.)} \pm 0.31 \text{ (extr.) mb,}$$

where the first error is statistical, the second accounts for all experimental systematic uncertainties and the last is related to uncertainties in the extrapolation $t \rightarrow 0$. In addition, the slope of the exponential function describing the elastic cross section at small t is determined to be $B = 19.74 \pm 0.05 \text{ (stat.)} \pm 0.23 \text{ (syst.) GeV}^{-2}$.

© 2016 The Author. Published by Elsevier B.V. This is an open access article under the CC BY license (<http://creativecommons.org/licenses/by/4.0/>). Funded by SCOAP³.

1. Introduction

The total cross section for proton–proton (pp) interactions characterizes a fundamental process of the strong interaction. Its energy evolution has been studied at each new range of centre-of-mass energies available. ATLAS has previously reported a measurement of the total cross section in pp collisions at $\sqrt{s} = 7$ TeV [1]. This paper details a measurement of the total cross section at $\sqrt{s} = 8$ TeV using data collected in 2012. The measurement methodology and analysis technique are very similar between the two measurements and the technical details are discussed thoroughly in Ref. [1].

Both measurements rely on the optical theorem:

$$\sigma_{\text{tot}} = 4\pi \text{Im} [f_{\text{el}}(t \rightarrow 0)] \quad (1)$$

which relates the total pp cross section σ_{tot} to the elastic-scattering amplitude extrapolated to the forward direction $f_{\text{el}}(t \rightarrow 0)$, with t being the four-momentum transfer squared. The total cross section can be extracted in different ways using the optical theorem. ATLAS uses the *luminosity-dependent* method which requires a measurement of the luminosity in order to normalize the elastic cross section. Here the measurement benefits from the high-precision luminosity measurement that ATLAS provides. With this method, σ_{tot} is given by the formula:

$$\sigma_{\text{tot}}^2 = \frac{16\pi(\hbar c)^2}{1 + \rho^2} \left. \frac{d\sigma_{\text{el}}}{dt} \right|_{t \rightarrow 0}, \quad (2)$$

where ρ represents a small correction arising from the ratio of the real to the imaginary part of the elastic-scattering amplitude in the forward direction and is taken from global model extrapolations [2].

The first measurement of σ_{tot} at the LHC at 8 TeV was performed by the TOTEM Collaboration [3] using a *luminosity-independent* method and using data from the same LHC fill as ATLAS. At 7 TeV measurements of σ_{tot} were provided by TOTEM [4–6] and ATLAS [1]. In a recent publication a measurement in the Coulomb–nuclear interference region at very small t was also reported by TOTEM [7]. The inelastic cross section σ_{inel} can either be derived from the total and elastic cross section measurements as in Refs. [3–6,1] at 7 and 8 TeV, or be determined directly from the measurement of the inelastic rate without exploiting the optical theorem. These measurements of σ_{inel} were performed at 7 TeV by all LHC Collaborations [8–12] and recently also at 13 TeV by ATLAS [13].

2. Experimental setup

The ATLAS detector is described in detail elsewhere [14]. The elastic-scattering data were recorded with the ALFA sub-detector (Absolute Luminosity For ATLAS) [1]. It consists of Roman Pot (RP) tracking-detector stations placed at distances of 237 m (inner sta-

* E-mail address: atlas.publications@cern.ch.

tion) and 241 m (outer station) on either side of the ATLAS interaction point (IP). Each station houses two vertically moveable scintillating fibre detectors which are inserted in RPs and positioned close to the beam for data taking. Each detector consists of 10 modules of scintillating fibres with 64 fibres on both the front and back sides of a titanium support plate. The fibres are arranged orthogonally in a u - v -geometry at $\pm 45^\circ$ with respect to the y -axis.¹ The spatial resolution of the detectors is about 35 μm . Elastic scattering events are recorded in two independent arms of the spectrometer. Arm 1 consists of two upper detectors at the left side and two lower detectors at the right side, and arm 2 consists inversely of two lower detectors at the left and two upper detectors at the right side. Events with reconstructed tracks in all four detectors of an arm are referred to as “golden” events [1]. The detectors are supplemented with trigger counters consisting of plain scintillator tiles. The detector geometry is illustrated in Fig. 1 of Ref. [1]. All scintillation signals are detected by photomultipliers coupled to a compact assembly of front-end electronics including the MAROC chip [15,16] for signal amplification and discrimination. The entire experimental setup is depicted in Fig. 2 of Ref. [1].

3. Experimental method

3.1. Measurement principle

The data were recorded in a single run of the LHC with special beam optics [17,18] of $\beta^* = 90 \text{ m}$.² The same optics were used at 7 TeV [1] and result in a small beam divergence with parallel-to-point focusing in the vertical plane. The four-momentum transfer t is calculated from the scattering angle θ^* and the beam momentum p by:

$$-t = (\theta^* \times p)^2, \quad (3)$$

where for the nominal beam momentum $p = 3988 \pm 26 \text{ GeV}$ is assumed [19] and the scattering angle is calculated from the proton trajectories and beam optics parameters. The relevant beam optics parameters are incorporated in transport matrix elements which describe the particle trajectory from the interaction point through the magnetic lattice of the LHC to the RPs. Several methods were developed for the reconstruction of the scattering angle, as detailed in Ref. [1]. The *subtraction method* has the best resolution and is selected as the nominal method. It uses only the track positions ($w = \{x, y\}$) and the matrix element $M_{12} = \sqrt{\beta \times \beta^*} \sin \psi$, where ψ refers to the phase advance of the betatron function at the RP:

$$\theta_w^* = \frac{w_A - w_C}{M_{12,A} + M_{12,C}}. \quad (4)$$

Here A refers to the left side of the IP at positive z and C refers to the right side at negative z . Three alternative methods are defined in detail in Ref. [1]. The *local angle method* uses only the M_{22} matrix element and the track angle between the inner and outer detectors. The *local subtraction method* uses a combination of M_{11} and M_{12} matrix elements and both the local angle and track position. The *lattice method* also uses both track parameters and reconstructs the scattering angle by an inversion of the transport matrix. The alternative methods are used to impose constraints on the beam optics and to cross-check the subtraction method.

¹ ATLAS uses a right-handed coordinate system with its origin at the nominal IP in the centre of the detector and the z -axis along the beam pipe. The x -axis points from the IP to the centre of the LHC ring and the y -axis points upwards.

² The β -function determines the variation of the beam envelope around the ring and depends on the focusing properties of the magnetic lattice; its value at the IP is denoted by β^* .

3.2. Data taking

The low-luminosity, high β^* run had 108 colliding bunches with about 7×10^{10} protons per bunch, but only 3 well-separated bunches of low emittance were selected for triggering. Precise positioning of the RPs is achieved with a beam-based alignment procedure which determines the position of the RPs with respect to the proton beams by monitoring the rate of the LHC beam-loss monitors during the RP insertion. The data were collected with the RPs at a distance of approximately 7.5 mm from the beam centre, corresponding to 9.5 times the vertical beam width. The beam centre and width monitored by LHC beam position monitors and the ATLAS beam-spot measurement [20] were found to be stable to within 10 μm during the run. The beam emittance was derived from the width of the luminous region in conjunction with the beam optics. It was supplemented by direct measurement from ALFA in the vertical plane. The luminosity-weighted average of the emittance in the vertical plane was determined to be 1.6 μm for both beams and between 1.8 μm and 2.5 μm for beam 1 and beam 2 respectively in the horizontal plane. The emittance uncertainty is about 10%.

To trigger on elastic-scattering events a coincidence was required between the A- and C-sides, where on each side at least one trigger signal in a detector of the corresponding arm was required. The trigger efficiency was determined from a data stream recorded with looser conditions to be 99.9% with negligible uncertainty. The dead-time fraction of the data acquisition system (DAQ) for the selected period was 0.4%.

3.3. Track reconstruction and alignment

A well-reconstructed elastic-scattering event consists of local tracks from the proton trajectory in all four ALFA stations. The reconstruction method assumes that the protons pass through the fibre detector perpendicularly. The average multiplicity per detector is about 23 hits, where typically 18–19 are attributed to the proton trajectory while the remaining 4–5 hits are due to beam-related background, cross-talk and electronic noise. Tracks are reconstructed in several steps from the overlap area of the hit fibres and several selections are applied [1] in order to reject events with hadronic shower developments.

The precise detector positions with respect to the circulating beams are crucial inputs for the reconstruction of the proton kinematics. First, the distance between the upper and the lower detectors is determined by the use of dedicated ALFA overlap detectors which allow simultaneous measurements of the same particle in the upper and lower half of a station. Then, the detector positions are directly determined from the elastic-scattering data, using the fact that the high- β^* optics and the azimuthal symmetry of the scattering angle result in elastic hit patterns that have an ellipsoidal shape elongated in the vertical direction. Three alignment parameters are determined for each detector: the horizontal and vertical offsets and the rotation angle around the beam axis. For the horizontal offset the centre of the x -distribution is taken and the rotation is obtained from a linear fit to a profile histogram of the x - y correlation. The vertical offset is obtained from a comparison of the yields in the upper and lower detectors using the sliding window technique [1]. The above procedures provide an independent alignment of each ALFA station. The vertical alignment parameters are in addition fine-tuned, exploiting the strong correlations between positions of tracks measured by different detectors in elastic events. First, the positions measured in one detector are extrapolated to the other detectors in the same arm using the ratio of the appropriate M_{12} matrix elements. Then, the extrapolated positions are compared to the corresponding measurements – the

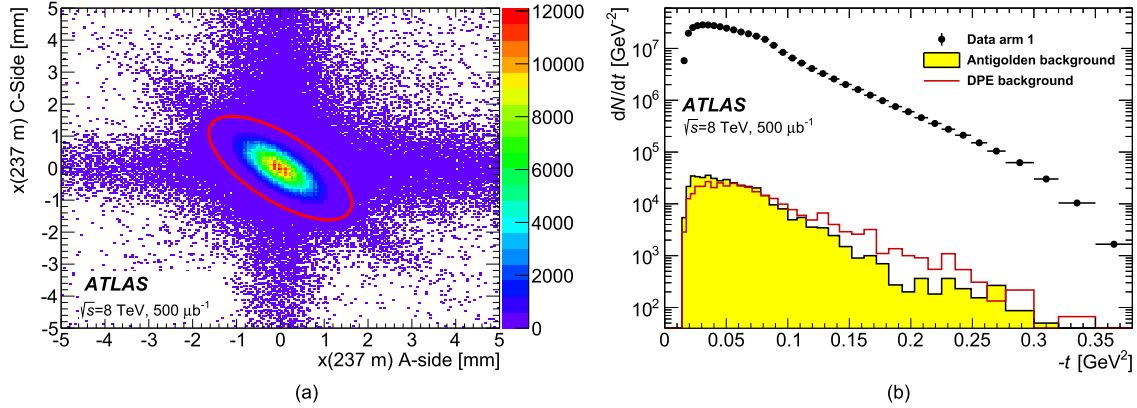


Fig. 1. (a) The correlation between the horizontal coordinates on the A- and C-sides. Elastic-scattering candidates after data quality, trigger and bunch selection but before acceptance and background rejection cuts are shown. Identified elastic events are required to lie inside the ellipse. (b) The distribution dN/dt , before corrections, as a function of t in arm 1 compared to the background spectrum determined using anti-golden events. The results of a simulation of the DPE background is also shown for comparison.

average distance gives information about residual misalignments. The residuals obtained for all pairs of detectors are combined with the vertical offset and distance measurements in a global χ^2 fit, resulting in the final alignment parameters.

4. Model for elastic scattering simulation

Several parameterizations are available [21–31] for the differential elastic pp cross section. A conventional approach is adopted here by taking the following simplified formulae:

$$\frac{d\sigma}{dt} = \frac{1}{16\pi} \left| f_N(t) + f_C(t)e^{i\alpha\phi(t)} \right|^2, \quad (5)$$

$$f_C(t) = -8\pi\alpha\hbar c \frac{G^2(t)}{|t|}, \quad (6)$$

$$f_N(t) = (\rho + i) \frac{\sigma_{\text{tot}}}{\hbar c} e^{-B|t|/2}, \quad (7)$$

where G is the electric form factor of the proton, B the nuclear slope, f_C the Coulomb amplitude and f_N the nuclear amplitude with ϕ their relative phase shift. The value of $\rho = \text{Re}(f_{el})/\text{Im}(f_{el}) = 0.1362 \pm 0.0034$ is taken from a global fit to lower-energy data [2] and parameterizations for G and ϕ are given in Ref. [1]. This expression is used to fit the data and extract σ_{tot} and B .

Monte Carlo simulation of elastic-scattering events is performed with PYTHIA8 [32,33] version 8.186 with a t -spectrum generated according to Eq. (5). The simulation is used to calculate acceptance and unfolding corrections. In the simulation the angular divergence of beams at the IP and the spread of the production vertex are set to the measured values. Elastically scattered protons are transported from the interaction point to the RPs nominally by means of the transport matrix. For studies of systematic uncertainties this was also done by the tracking module of the MadX [34] beam optics calculation program. A fast parameterization of the detector response is used in the simulation and tuned to reproduce the measured difference in position between the outer detectors and their position as extrapolated from the inner detectors.

5. Data analysis

5.1. Event selection

Events are required to pass the trigger conditions for elastic-scattering events and have a reconstructed track in all four detectors of an arm in the golden topology. The fiducial volume is

defined by cuts on the vertical coordinate of the reconstructed track, which is required to be at least $90 \mu\text{m}$ from the detector edge near the beam and at least 1 mm away from the shadow of the beam screen, in each of the four detectors.³ The values of cuts are chosen to obtain good agreement between data and simulation in the position distributions. The back-to-back topology of elastic events is further exploited to clean the sample by imposing cuts on the left-right acollinearity. The difference between the absolute value of the vertical coordinate at the A- and C-side is requested to be below 3 mm . For the horizontal coordinate the correlation of the A- and C-sides is used. Events are selected inside an ellipse with half-axis values of 3.5σ of the resolution determined by simulation, as illustrated in Fig. 1(a). Elastic events are concentrated inside a narrow ellipse with negative slope, whereas the beam-halo background appears in broad uncorrelated bands. The most efficient selection against background is obtained from the correlation between the position in the horizontal plane and the local angle between two stations, where events on either side are again required to be inside an ellipse of 3.5σ width. From an initial sample of 4.2 million elastic candidates, 3.8 million golden elastic events were selected after all cuts. The t -spectrum, before corrections, for selected elastic events in one arm is shown in Fig. 1(b).

5.2. Background estimate

A small fraction of the events inside the selected elliptical area shown in Fig. 1(a) are expected to be background, predominantly originating from double-Pomeron exchange (DPE) according to simulations based on the MBR model [35]. The background is estimated with a data-driven method [1] using events in the “anti-golden” topology with two tracks in both upper or both lower detectors at the A- and C-sides. This sample is free of signal and yields an estimate of background in the elastic sample with the golden topology. The shape of the t -spectrum for background events is obtained by flipping the sign of the vertical coordinate on either side. The resulting background distribution is shown in Fig. 1(b). In total 4400 background events are estimated to be in the selected sample, corresponding to a fraction of 0.12% of the selected events. The systematic uncertainty is about 50%, as derived in Ref. [1] from a comparison of different methods.

³ The beam screen is a protection element of the quadrupoles, which limits the acceptance of the detector at large $|y|$.

5.3. Reconstruction efficiency

The rate of elastic-scattering events is corrected for reconstruction inefficiencies. These events may not be reconstructed when protons or halo particles interact with the stations or detectors, causing a shower to develop and resulting in high fibre hit multiplicities. This correction is called the event reconstruction efficiency and is given by

$$\varepsilon_{\text{rec}} = \frac{N_{\text{reco}}}{N_{\text{reco}} + N_{\text{fail}}}, \quad (8)$$

for each arm where N_{reco} is the number of reconstructed events and N_{fail} the number of events for which the reconstruction failed because a shower developed. The sample of failed events is split into different categories depending on the number of detectors with reconstruction failures, because the event background is different for each category. The fraction of elastic events in the subsample where one out of four detectors failed to reconstruct a track is above 99%, whereas this fraction is 95% for the subsample where two detectors failed to reconstruct a track on one side. The event yields in the different categories are calculated with a data-driven method, for which the details are given in Ref. [1]. The background fraction in the case with only two detectors with reconstructed tracks is estimated with background templates of the x distribution, obtained from data by selecting single diffractive events. In the case of a successful track reconstruction in three detectors, where a good t -measurement is still possible, the partial reconstruction efficiency was verified to be independent of t , which is then also assumed for the other categories. Events falling outside the acceptance, but faking a signal through shower development, were eliminated from the reconstruction efficiency calculation by applying another template analysis using the y distribution obtained from golden elastic events.

The event reconstruction efficiencies in arm 1 and arm 2 are determined to be $\varepsilon_{\text{rec},1} = 0.9050 \pm 0.0003$ (stat.) ± 0.0034 (syst.) and $\varepsilon_{\text{rec},2} = 0.8883 \pm 0.0003$ (stat.) ± 0.0045 (syst.), respectively. The lower reconstruction efficiency in arm 2 originates from a different amount of material which induces a higher probability of shower development. The systematic uncertainty is estimated by a variation of the selection criteria and templates, as described in Ref. [1].

5.4. Beam optics

The precision of the t -reconstruction depends on knowledge of the transport matrix elements. A data-driven method was developed [1] to tune the relevant matrix elements using constraints on the beam optics derived from measured correlations in the ALFA data. These constraints are incorporated in a fit of the strength of the inner triplet quadrupole magnets Q1 and Q3, which yields an effective beam optics used in the simulation. The values of the constraints are compatible with those published in Ref. [1] within 15% and the resulting magnet strength offsets are in good agreement with the values found at 7 TeV.

5.5. Acceptance and unfolding

The acceptance is defined as the ratio of events passing all geometrical and fiducial acceptance cuts to all generated events, and is calculated as a function of t . The form of the acceptance curve as shown in Fig. 2 results from the different contributions of the vertical and horizontal scattering angles to the value of t and the impact of the fiducial volume cuts on these contributions. In particular, the position of the peak depends on the cut at large $|y|$ at the beam screen, which is slightly different for the two arms. The

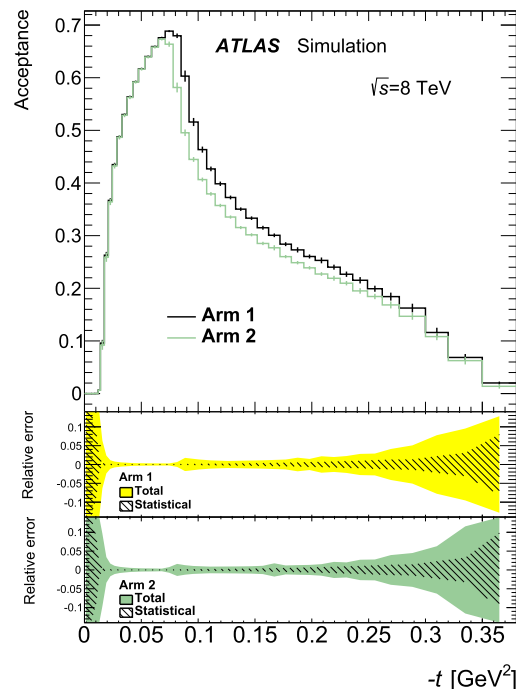


Fig. 2. The acceptance as a function of the true value of t for each arm with total uncertainties shown as error bars. The lower panels show relative total and statistical uncertainties.

rise of the acceptance at small t is different in the two arms because of different detector distances, between 8 and 8.4 mm, to the beam.

The measured t -spectrum is affected by detector resolution and beam divergence effects, which are corrected with an unfolding procedure. The t -resolution of the subtraction method is about 10% at small t and 3% at large t . The alternative methods have a t -resolution which is a factor of 2–3 worse [1]. The background-subtracted distributions in each arm are corrected for migration effects using an iterative, dynamically stabilized, unfolding method [36], which is based on a simulated transition matrix describing the resolution-induced migration between bins of the t -spectrum. The corrections induced by the unfolding are small (<2%) for the subtraction method except at small t where they rise to 30%. For the other methods the corrections are generally t -dependent and increase to 50% at large t .

5.6. Luminosity

The ATLAS luminosity measurement at high luminosity ($L > 10^{33}$ cm⁻² s⁻¹) is described in detail in Ref. [37]. Unlike that measurement, the run in this analysis had an instantaneous luminosity $L \sim 0.05 \cdot 10^{30}$ cm⁻² s⁻¹, about five orders of magnitude lower. Only three bunches were present in this run, whereas more than a thousand bunches are common at high luminosity. The average number of interactions per bunch-crossing (pile-up) in this sample is $\mu \sim 0.1$, which is also low compared to the values of $\mu = 10$ –40 reached routinely in normal conditions. At such low values of the luminosity, some of the standard algorithms are unusable due to lack of sensitivity. On the other hand, an additional method based on vertex counting in the inner detector (ID) can be exploited, which is most effective at low pile-up. Another consequence of the low luminosity is the relative importance of the background sources: the beam-gas contribution, normally negligible, can become comparable with the collision rate, while the “afterglow”

background (see Ref. [37]) becomes conversely less important, due to the small number of colliding bunches.

In 2012, the beam conditions monitor (BCM) was used as the baseline detector for luminosity measurements. It consists of diamond-sensor detectors placed on both sides of the IP. It measures the luminosity using an event-counting method based on the requirement of having activity in either side (BCM_EventOR). LUCID (LUminosity measurement with a Cherenkov Integrating Detector) is also located on both sides of the IP and uses the same algorithm to measure the luminosity (LUCID_EventOR). A third method for measuring the per-bunch luminosity is provided by the ID. Tracks are reconstructed requiring at least nine hits and no missing hits along the track trajectory, and a transverse momentum $p_T > 900$ MeV. Then, at least five selected tracks are required to form a primary vertex (VTX5). The number of primary vertices per event is proportional to the luminosity and provides an independent method with respect to LUCID and BCM.

The absolute luminosity scale of each algorithm was calibrated by the van der Meer (vdM) method [38] at an intermediate luminosity regime ($L \sim 10^{30} \text{ cm}^{-2} \text{ s}^{-1}$). The treatment of both afterglow and beam-gas background is described in detail in Ref. [37]. The first is evaluated by measuring the detector activity in unfilled bunches preceding the colliding bunches, while the second is estimated from the so-called unpaired bunches, in which bunches in only one of the two beams are filled and no beam-beam collisions occur. In the high- β^* run and for BCM_EventOR, the afterglow background is evaluated to be 0.05% and the beam-gas contribution is 0.4%.

BCM_EventOR was chosen as the baseline algorithm for the luminosity determination, whereas the LUCID_EventOR and VTX5 methods are only used for the evaluation of systematic uncertainties. It proved to be the most stable, both by comparing the various vdM calibration sessions performed during the year and by studying its long-term behaviour at high luminosity. This choice also ensures maximum compatibility with the high-luminosity case. By comparing the LUCID_EventOR and VTX5 results with BCM_EventOR, a maximum difference of 0.3% is found. No change of this difference with time, or equivalently μ , is observed.

The following contributions to the systematic uncertainty of the luminosity determination are considered:

- The absolute luminosity scale, common to all algorithms, is determined by the vdM method. Its uncertainty of 1.2% is dominated by the beam conditions. This uncertainty is fully correlated between low- and high-luminosity data sets [37].
- The BCM calibration stability between the high- β^* run and the vdM session is estimated to be 0.8% by comparing with the VTX5 method among the various vdM scans.
- The afterglow background uncertainty is conservatively taken as 100% of the afterglow level itself, which leads to an uncertainty of 0.05% in the luminosity.
- The beam-gas background uncertainty is obtained using LUCID by comparing the difference in the off-time activity (i.e. produced by beam-gas interactions and not by collisions at the IP) between the colliding and the unpaired bunches. It is estimated to be 0.3%.

The total systematic uncertainty is therefore 1.5%. The final integrated luminosity is measured to be $L_{\text{int}} = 496.3 \pm 0.3$ (stat.) ± 7.3 (syst.) μb^{-1} .

6. Results

6.1. Elastic cross section

The differential elastic cross section in a given bin t_i is calculated from the following formula:

$$\frac{d\sigma_{\text{el}}}{dt_i} = \frac{1}{\Delta t_i} \times \frac{\mathcal{M}^{-1}[N_i - B_i]}{A_i \times \epsilon^{\text{reco}} \times \epsilon^{\text{trig}} \times \epsilon^{\text{DAQ}} \times L_{\text{int}}}, \quad (9)$$

where Δt_i is the width of the bins in t , \mathcal{M}^{-1} symbolizes the unfolding procedure applied to the background-subtracted number of events $N_i - B_i$, A_i is the acceptance, ϵ^{reco} is the event reconstruction efficiency, ϵ^{trig} is the trigger efficiency, ϵ^{DAQ} is the dead-time correction and L_{int} is the integrated luminosity. The binning in t is chosen to yield a purity above 50%, which corresponds to 1.5 times the resolution at small t . It is enlarged at large t in order to account for the lower number of events. The numerical values for the resulting differential elastic cross section are given in Table 1.

The experimental systematic uncertainties are derived according to the methods detailed in Ref. [1] as follows:

- The value of the beam momentum used in the t -reconstruction (Eq. (3)) and in the simulation is varied by 0.65%, as recommended in Ref. [19].
- The uncertainty in the luminosity of 1.5% is applied to the cross-section normalization.
- The event reconstruction efficiency is varied by its uncertainty of about 0.5% and the uncertainty in the tracking efficiency is estimated by varying the reconstruction criteria.
- The uncertainties originating from the effective beam optics are calculated from variations of the optics constraints, of the strength of the quadrupoles not adjusted in the fit, and of the quadrupole alignment constants. Additional uncertainties are related to the error of the optics fit, to the beam transport scheme used in the simulation, and to the impact from a residual beam crossing angle assumed to vary within its uncertainty of $\pm 10 \mu\text{rad}$.
- The uncertainties from the alignment of the ALFA detectors are evaluated by varying the correction constants for horizontal and vertical offsets as well as the rotation within their uncertainties as determined from variations of the alignment procedures, and by taking the difference between different optimization configurations for the vertical alignment parameters.
- The background normalization uncertainty of 50% is applied in the background subtraction and the background shape is varied by inverting the sign of different detector combinations.
- The detector resolution values in the fast simulation are replaced by estimates from GEANT4 [39,40] and test-beam measurements, and a y -dependent resolution is used instead of a constant value.
- The value of the nuclear slope in the simulation is varied around the nominal value of 19.7 GeV^{-2} by $\pm 1 \text{ GeV}^{-2}$, corresponding to about five times the uncertainty of the measured B value.
- The beam emittance value in the simulation is varied by its uncertainty of about 7%. Additionally, the ratio of the emittance in beam 1 to the emittance in beam 2, which are measured by wire scans after injection only, is set to unity.
- The intrinsic unfolding uncertainty is estimated from a data-driven closure test.

The main sources of systematic uncertainty are the beam momentum uncertainty and the luminosity uncertainty. For each system-

Table 1

The measured values of the differential elastic cross section with statistical and systematic uncertainties. The central t -values in each bin are calculated from simulation, in which a slope parameter of $B = 19.7 \text{ GeV}^{-2}$ is used.

Low $ t $ edge [GeV ²]	High $ t $ edge [GeV ²]	Central $ t $ [GeV ²]	$d\sigma_{el}/dt$ [mb/GeV ²]	Stat. uncert. [mb/GeV ²]	Syst. uncert. [mb/GeV ²]	Total uncert. [mb/GeV ²]
0.0090	0.0120	0.0105	387	29	14	32
0.0120	0.0140	0.0130	370	5.6	12	13
0.0140	0.0175	0.0157	352.3	1.4	8.7	8.9
0.0175	0.0210	0.0192	329.8	0.8	6.5	6.5
0.0210	0.0245	0.0227	306.9	0.6	5.7	5.8
0.0245	0.0285	0.0265	284.6	0.5	5.0	5.1
0.0285	0.0330	0.0307	261.7	0.4	4.6	4.6
0.0330	0.0375	0.0352	239.3	0.4	4.1	4.1
0.0375	0.0425	0.0400	218.0	0.4	3.6	3.6
0.0425	0.0475	0.0450	197.3	0.3	3.3	3.3
0.0475	0.0530	0.0502	178.0	0.3	3.0	3.0
0.0530	0.0590	0.0559	158.8	0.2	2.7	2.7
0.0590	0.0650	0.0619	141.1	0.2	2.4	2.4
0.0650	0.0710	0.0679	126.0	0.2	2.2	2.2
0.0710	0.0780	0.0744	111.1	0.2	2.0	2.0
0.0780	0.0850	0.0814	96.8	0.2	2.0	2.0
0.0850	0.0920	0.0884	84.7	0.2	1.7	1.7
0.0920	0.1000	0.0959	72.9	0.2	1.6	1.6
0.1000	0.1075	0.1037	62.7	0.2	1.5	1.5
0.1075	0.1150	0.1112	54.1	0.2	1.3	1.4
0.1150	0.1240	0.1194	46.11	0.14	1.13	1.13
0.1240	0.1330	0.1284	38.76	0.14	1.0	1.01
0.1330	0.1420	0.1374	32.60	0.12	0.92	0.93
0.1420	0.1520	0.1468	27.10	0.11	0.82	0.83
0.1520	0.1620	0.1568	22.48	0.11	0.74	0.74
0.1620	0.1720	0.1668	18.48	0.10	0.68	0.68
0.1720	0.1820	0.1768	15.25	0.09	0.67	0.68
0.1820	0.1930	0.1873	12.36	0.08	0.57	0.58
0.1930	0.2030	0.1978	10.08	0.08	0.48	0.48
0.2030	0.2140	0.2083	8.20	0.07	0.43	0.43
0.2140	0.2250	0.2193	6.58	0.06	0.33	0.33
0.2250	0.2360	0.2303	5.34	0.06	0.27	0.28
0.2360	0.2490	0.2422	4.28	0.05	0.24	0.24
0.2490	0.2620	0.2552	3.30	0.05	0.22	0.23
0.2620	0.2770	0.2691	2.47	0.04	0.18	0.18
0.2770	0.3000	0.2877	1.69	0.03	0.14	0.14
0.3000	0.3200	0.3094	1.06	0.03	0.10	0.1
0.3200	0.3500	0.3335	0.62	0.02	0.08	0.08
0.3500	0.3800	0.3635	0.36	0.04	0.04	0.05

atic uncertainty source the shift of the cross-section value in each t -bin is recorded. The most important shifts are shown in Fig. 3(a).

6.2. Total cross section

A profile fit [41] is used to determine σ_{tot} . It includes statistical and systematic uncertainties and their correlations across the t -spectrum. For each shift due to a systematic uncertainty a nuisance parameter is fitted in a procedure described in Ref. [1].

The theoretical prediction of Eq. (5) including the Coulomb and interference terms is fitted to the data to extract σ_{tot} and B alongside the nuisance parameters, as shown in Fig. 3(b). The fit range is chosen to be from $-t = 0.014 \text{ GeV}^2$ to $-t = 0.1 \text{ GeV}^2$, where the lower bound is set by requiring the acceptance to exceed 10% and the upper bound is chosen to exclude the large- t region where theoretical models predict deviations from a single exponential function [42]. The fit yields $\sigma_{\text{tot}} = 96.07 \pm 0.86 \text{ mb}$ and $B = 19.74 \pm 0.17 \text{ GeV}^{-2}$ with $\chi^2/N_{\text{dof}} = 17.8/14$ and the uncertainties include all statistical and experimental systematic contributions. The most important uncertainty component is the luminosity error for σ_{tot} and the beam energy error for B . Additional uncertainties arising from the extrapolation $t \rightarrow 0$ are estimated from a variation of the upper end of the fit range respectively up to $-t = 0.152 \text{ GeV}^2$ and up to $-t = 0.065 \text{ GeV}^2$, and from a variation of the lower end, i.e. from $-t = 0.009 \text{ GeV}^2$ to $-t = 0.0245 \text{ GeV}^2$. Further theoretical uncertainties considered

include: a variation of the ρ -parameter in Eq. (1) by ± 0.0034 ; the replacement of the dipole parameterization by a double-dipole parameterization [43] for the proton electric form factor; the replacement of the Coulomb phase from West and Yennie [22] by parameterizations from Refs. [24,27]; the inclusion of a term related to the magnetic moment of the proton in the Coulomb amplitude [23]. The dominant extrapolation uncertainty is induced by the fit range variation. The final results for σ_{tot} and B are:

$$\sigma_{\text{tot}} = 96.07 \pm 0.18 \text{ (stat.)} \pm 0.85 \text{ (exp.)} \pm 0.31 \text{ (extr.) mb}, \quad (10)$$

$$B = 19.74 \pm 0.05 \text{ (stat.)} \pm 0.16 \text{ (exp.)} \pm 0.15 \text{ (extr.) GeV}^{-2}. \quad (11)$$

A summary of the results for σ_{tot} from four different t -reconstruction methods is given in Table 2. The results from the nominal subtraction method are in good agreement with the other methods, considering the uncorrelated uncertainty of 0.3–0.4 mb. The alternative methods are correlated through the common use of the local angle variable.

Further stability checks are carried out in order to cross-check the fitting method. A fit using only the covariance matrix of statistical uncertainties yields $\sigma_{\text{tot}} = 96.34 \pm 0.07 \text{ (stat.)}$ in good agreement with the results from the profile fit Eq. (10). The same fit with only statistical uncertainties was also performed for the two arms of ALFA independently and gave consistent results within one standard deviation of the statistical uncertainty. The data sample was split into ten sub-periods with roughly equal numbers of selected events and no dependence of the measured value of σ_{tot} on

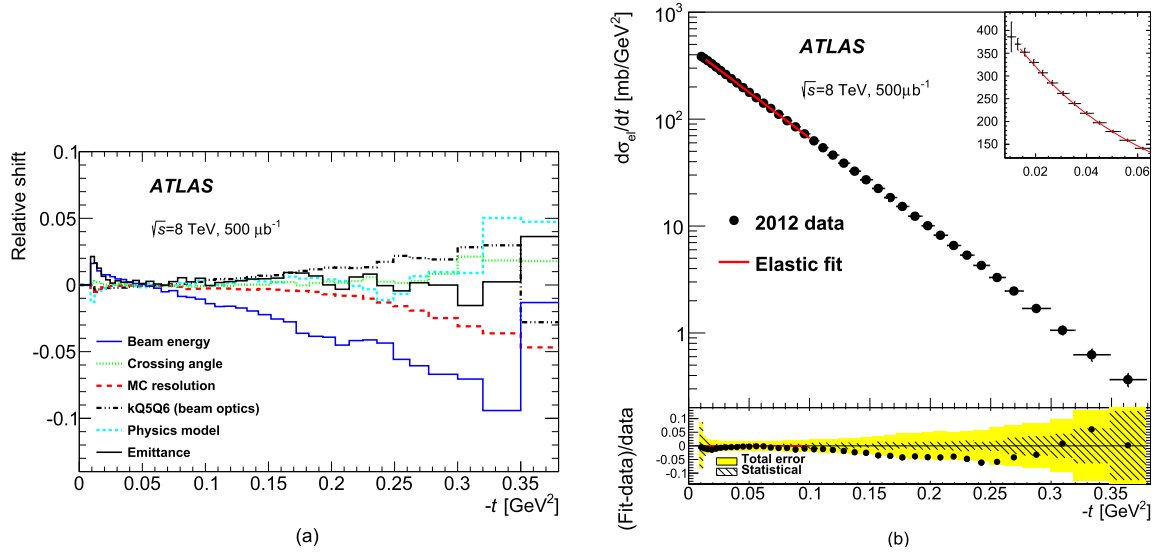


Fig. 3. (a) Relative shifts in the differential elastic cross section as a function of t for selected systematic uncertainty sources. Shown are the uncertainties related to the beam energy, to the crossing angle, to the modelling of the detector resolution in the simulation (MC resolution), to the beam optics (kQ5Q6, magnet strength), to the value of B in the simulation (Physics model) and to the emittance. (b) The fit of the theoretical prediction to the differential elastic cross section with σ_{tot} and B as free parameters. In the lower plot the points represent the relative difference between fit and data, the yellow area represents the total experimental uncertainty and the hatched area the statistical component. The red line indicates the fit range; the fit result is extrapolated in the lower plot outside the fit range. The upper right insert shows a zoom of the data and fit at small t . (For interpretation of the references to colour in this figure legend, the reader is referred to the web version of this article.)

Table 2

The total cross section and uncertainties for four different t -reconstruction methods. The nominal results are based on the subtraction method, quoted in the second column.

	σ_{tot} [mb]			
	Subtraction	Local angle	Lattice	Local subtraction
Total cross section	96.07	96.52	96.56	96.58
Statistical error	0.18	0.15	0.16	0.15
Experimental error	0.85	0.94	0.88	0.89
Extrapolation error	0.31	0.42	0.23	0.23
Total error	0.92	0.98	0.93	0.93

time was observed. Also, the data from the three different bunches were investigated independently and found to give consistent results. Finally the stability of the analysis was tested by a wide variation of the event selection cuts. The largest change of σ_{tot} with these cut variations was observed for the cut on the correlation between x and θ_x . That produced a change of ± 0.3 mb, well within the t -dependent experimental systematic uncertainty of about 0.5 mb. Several alternative parameterizations [22,26,28,27,29–31] of the differential elastic cross section, including non-exponential forms at large t , were used to fit the spectrum up to $-t = 0.3 \text{ GeV}^2$ in order to assess the impact on the value of the total cross section. The RMS of the values obtained is 0.28 mb, in good agreement with the quoted extrapolation uncertainty of 0.31 mb assigned to the simple exponential form.

The TOTEM Collaboration exploited data from the same LHC fill for a measurement of σ_{tot} using the luminosity-independent method. Their result is $\sigma_{\text{tot}} = 101.7 \pm 2.9 \text{ mb}$ [3], higher than the measurement presented here. The difference corresponds to 1.9σ assuming uncorrelated uncertainties. Better agreement is observed in the nuclear slope measurement, where TOTEM reports $B = 19.9 \pm 0.3 \text{ GeV}^{-2}$, a value very close to the present result $B = 19.74 \pm 0.19 \text{ GeV}^{-2}$, which indicates that the difference is confined to the normalization. The measurements of ATLAS and TOTEM are compared to measurements at lower energy and to a global fit [2] in Fig. 4(a) for σ_{tot} and in Fig. 4(b) for B . TOTEM also reported evidence of non-exponential behaviour of the differential

elastic cross section [49] in the $-t$ -range below 0.2 GeV^2 , where deviations from the single exponential form of the order of one percent are observed. Such effects cannot be substantiated with this data set because their size is below the systematic uncertainties of the present measurement.

As well as the total cross section, the total integrated elastic cross section can be calculated, provided that the Coulomb amplitude is neglected. In this case, σ_{el} can be obtained from the formula

$$\sigma_{\text{el}} = \frac{\sigma_{\text{tot}}^2}{B} \frac{1 + \rho^2}{16\pi (\hbar c)^2}, \quad (12)$$

and the result is $\sigma_{\text{el}} = 24.33 \pm 0.04$ (stat.) ± 0.39 (syst.) mb. The measured integrated elastic cross section in the fiducial range from $-t = 0.009 \text{ GeV}^2$ to $-t = 0.38 \text{ GeV}^2$ corresponds to 80% of this total elastic cross section $\sigma_{\text{el}}^{\text{observed}} = 19.67 \pm 0.02$ (stat.) ± 0.33 (syst.) mb. The total inelastic cross section is determined by subtraction of the total elastic cross section from the total cross section. The resulting value is $\sigma_{\text{inel}} = 71.73 \pm 0.15$ (stat.) ± 0.69 (syst.) mb.

7. Conclusion

ATLAS has performed a measurement of the total cross section from elastic pp scattering at $\sqrt{s} = 8 \text{ TeV}$. The measurement is based on $500 \mu\text{b}^{-1}$ of collision data collected in a high- β^* run at the LHC in 2012 with the ALFA Roman Pot sub-detector. The optical theorem is used to extract the total cross section from the differential elastic cross section by extrapolating $t \rightarrow 0$. The differential cross section is also used to determine the nuclear slope. The analysis uses data-driven methods to determine relevant beam optics parameters and event reconstruction efficiency, and to tune the simulation. The detailed evaluation of the associated systematic uncertainties is supplemented by a comparison of t -reconstruction methods with different sensitivities to beam optics. The absolute luminosity for this run is determined in a dedicated analysis, taking into account the special conditions with a very low number of interactions per bunch crossing. The total cross section at $\sqrt{s} = 8 \text{ TeV}$ is determined to be

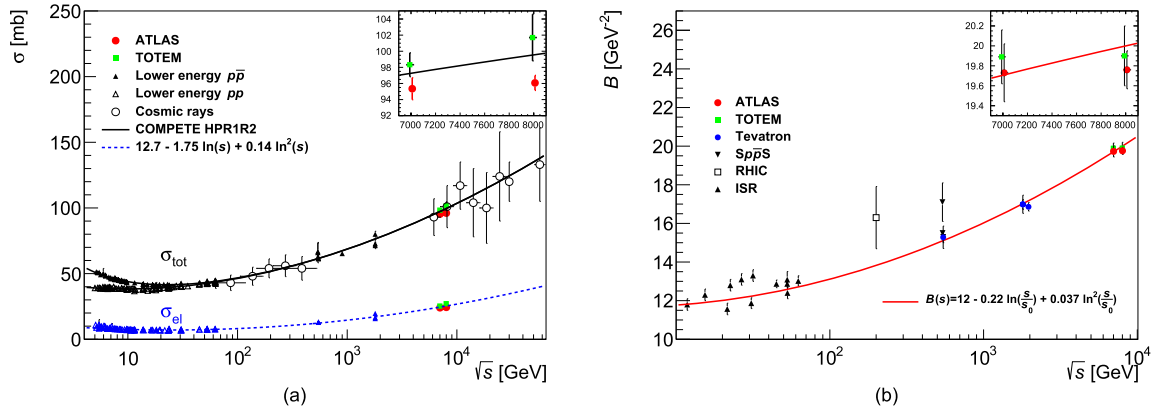


Fig. 4. (a) Comparison of total and elastic cross-section measurements presented here with other published measurements [2,5,44–47] and model predictions as a function of the centre-of-mass energy. (b) Comparison of the measurement of the nuclear slope B presented here with other published measurements at the ISR, at the $Sp\bar{p}S$, at RHIC, at the Tevatron and with the measurement from TOTEM at the LHC. The red line shows a model calculation [48], which contains a linear term and quadratic term in $\ln s$. (For interpretation of the references to colour in this figure legend, the reader is referred to the web version of this article.)

$$\sigma_{tot}(pp \rightarrow X) = 96.07 \pm 0.18 \text{ (stat.)} \pm 0.85 \text{ (exp.)} \\ \pm 0.31 \text{ (extr.) mb,}$$

where the first error is statistical, the second accounts for all experimental systematic uncertainties and the last is related to uncertainties in the extrapolation $t \rightarrow 0$. In addition, the slope of the elastic differential cross section at small t is determined to be $B = 19.74 \pm 0.05 \text{ (stat.)} \pm 0.23 \text{ (syst.) GeV}^{-2}$.

The total elastic cross section is extracted from the fitted parameterization as $\sigma_{el}(pp \rightarrow pp) = 24.33 \pm 0.04 \text{ (stat.)} \pm 0.39 \text{ (syst.) mb}$ and the inelastic cross section is obtained by subtraction from the total cross section as $\sigma_{inel} = 71.73 \pm 0.15 \text{ (stat.)} \pm 0.69 \text{ (syst.) mb}$. The measurements at 8 TeV are significantly more precise than the previous measurements at 7 TeV because of the smaller luminosity uncertainty and a larger data sample.

Acknowledgements

We thank CERN for the very successful operation of the LHC, as well as the support staff from our institutions without whom ATLAS could not be operated efficiently. We are indebted to the beam optics development team, led by H. Burkhardt, for the design, commissioning and thorough operation of the high- β^* optics in dedicated LHC fills.

We acknowledge the support of ANPCyT, Argentina; YerPhI, Armenia; ARC, Australia; BMWFW and FWF, Austria; ANAS, Azerbaijan; SSTC, Belarus; CNPq and FAPESP, Brazil; NSERC, NRC and CFI, Canada; CERN; CONICYT, Chile; CAS, MOST and NSFC, China; COLCIENCIAS, Colombia; MSMT CR, MPO CR and VSC CR, Czech Republic; DNRf and DNSRC, Denmark; IN2P3-CNRS, CEA-DSM/IRFU, France; GNSF, Georgia; BMBF, HGF, and MPG, Germany; GSRT, Greece; RGC, Hong Kong SAR, China; ISF, I-CORE and Benoziyo Center, Israel; INFN, Italy; MEXT and JSPS, Japan; CNRS, Morocco; FOM and NWO, Netherlands; RCN, Norway; MNiSW and NCN, Poland; FCT, Portugal; MNE/IFA, Romania; MES of Russia and NRC KI, Russian Federation; JINR; MESTD, Serbia; MSSR, Slovakia; ARRS and MIZŠ, Slovenia; DST/NRF, South Africa; MINECO, Spain; SRC and Wallenberg Foundation, Sweden; SERI, SNSF and Cantons of Bern and Geneva, Switzerland; MOST, Taiwan; TAEK, Turkey; STFC, United Kingdom; DOE and NSF, United States of America. In addition, individual groups and members have received support from BCKDF, the Canada Council, Canarie, CRC, Compute Canada, FQRT, and the Ontario Innovation Trust, Canada; EPLANET, ERC, FP7, Horizon 2020 and Marie Skłodowska-Curie Actions, European Union; Investissements d’Avenir Labex and Idex, ANR, Région Auvergne

and Fondation Partager le Savoir, France; DFG and AvH Foundation, Germany; Herakleitos, Thales and Aristeia programmes co-financed by EU-ESF and the Greek NSRF; BSF, GIF and Minerva, Israel; BRF, Norway; Generalitat de Catalunya, Generalitat Valenciana, Spain; the Royal Society and Leverhulme Trust, United Kingdom.

The crucial computing support from all WLCG partners is acknowledged gratefully, in particular from CERN, the ATLAS Tier-1 facilities at TRIUMF (Canada), NDGF (Denmark, Norway, Sweden), CC-IN2P3 (France), KIT/GridKA (Germany), INFN-CNAF (Italy), NL-T1 (Netherlands), PIC (Spain), ASGC (Taiwan), RAL (UK) and BNL (USA), the Tier-2 facilities worldwide and large non-WLCG resource providers. Major contributors of computing resources are listed in Ref. [50].

References

- [1] ATLAS Collaboration, Measurement of the total cross section from elastic scattering in pp collisions at $\sqrt{s} = 7$ TeV with the ATLAS detector, Nucl. Phys. B 889 (2014) 486, arXiv:1408.5778 [hep-ex].
- [2] K.A. Olive, et al., Particle Data Group, in: Review of Particle Physics, Chin. Phys. C 38 (2014) 090001.
- [3] G. Antchev, et al., TOTEM Collaboration, Luminosity-independent measurement of the proton–proton total cross section at $\sqrt{s} = 8$ TeV, Phys. Rev. Lett. 111 (2013) 012001.
- [4] G. Antchev, et al., TOTEM Collaboration, First measurement of the total proton–proton cross-section at the LHC energy of $\sqrt{s} = 7$ TeV, Europhys. Lett. 96 (2011) 21002, arXiv:1110.1395 [hep-ex].
- [5] G. Antchev, et al., TOTEM Collaboration, Measurement of proton–proton elastic scattering and total cross-section at $\sqrt{s} = 7$ TeV, Europhys. Lett. 101 (2013) 21002.
- [6] G. Antchev, et al., TOTEM Collaboration, Luminosity-independent measurements of total, elastic and inelastic cross-sections at $\sqrt{s} = 7$ TeV, Europhys. Lett. 101 (2013) 21004.
- [7] G. Antchev, et al., TOTEM Collaboration, Measurement of elastic pp scattering at $\sqrt{s} = 8$ TeV in the Coulomb-nuclear interference region – determination of the ρ parameter and the total cross-section, TOTEM-2015-002, CERN-PH-EP-2015-325, <http://cds.cern.ch/record/2114603>, 2015.
- [8] ATLAS Collaboration, Measurement of the inelastic proton–proton cross-section at $\sqrt{s} = 7$ TeV with the ATLAS detector, Nat. Commun. 2 (2011) 463, arXiv:1104.0326 [hep-ex].
- [9] CMS Collaboration, Measurement of the inelastic proton–proton cross section at $\sqrt{s} = 7$ TeV, Phys. Lett. B 722 (2013) 5–27, arXiv:1210.6718 [hep-ex].
- [10] R. Aaij, et al., LHCb Collaboration, Measurement of the inelastic pp cross-section at a centre-of-mass energy of $\sqrt{s} = 7$ TeV, J. High Energy Phys. 02 (2015) 129, arXiv:1412.2500 [hep-ex].
- [11] B. Abelev, et al., ALICE Collaboration, Measurement of inelastic, single- and double-diffraction cross sections in proton–proton collisions at the LHC with ALICE, Eur. Phys. J. C 73 (2013) 2456, arXiv:1208.4968 [hep-ex].
- [12] G. Antchev, et al., TOTEM Collaboration, Measurement of proton–proton inelastic scattering cross-section at $\sqrt{s} = 7$ TeV, Europhys. Lett. 101 (2013) 21003.

- [13] ATLAS Collaboration, Measurement of the inelastic proton–proton cross section at $\sqrt{s} = 13$ TeV with the ATLAS detector at the LHC, arXiv:1606.02625 [hep-ex], 2016.
- [14] ATLAS Collaboration, The ATLAS experiment at the CERN large hadron collider, *J. Instrum.* 3 (2008) S08003.
- [15] P. Barrillon, et al., PMF: the front end electronic of the ALFA detector, *Nucl. Instrum. Methods A* 623 (2010) 463.
- [16] S. Blin, P. Barrillon, C. de La Taille, MAROC, a generic photomultiplier readout chip, in: Proceedings of the 2010 IEEE Nuclear Science Symposium and Medical Imaging Conference, NSS/MIC 2010, 2010, p. 1690.
- [17] H. Burkhardt, et al., 90 m optics studies and operation in the LHC, *Conf. Proc. C* 1205201 (2012) 130.
- [18] H. Burkhardt, et al., 90 m Beta' optics for ATLAS/ALFA, *Conf. Proc. C* 110904 (2011) 1798.
- [19] J. Wenninger, Energy calibration of the LHC beams at 4 TeV, CERN-ATS-2013-040, <http://cds.cern.ch/record/1546734>, 2013.
- [20] ATLAS Collaboration, Characterization of interaction–point beam parameters using the pp event-vertex distribution reconstructed in the ATLAS Detector at the LHC, ATLAS-CONF-2010-027, <http://cdsweb.cern.ch/record/1277659>, 2010.
- [21] H.A. Bethe, Scattering and polarization of protons by nuclei, *Ann. Phys.* 3 (1958) 190.
- [22] G.B. West, D.R. Yennie, Coulomb interference in high-energy scattering, *Phys. Rev.* 172 (1968) 1413.
- [23] C. Bourrely, J. Soffer, D. Wray, Spin effects in proton–proton elastic scattering near the forward direction, *Nucl. Phys. B* 77 (1974) 386.
- [24] R.N. Cahn, Coulombic-hadronic interference in an Eikonal model, *Z. Phys. C* 15 (1982) 253.
- [25] M.J. Menon, P.V.R.G. Silva, A study on analytic parametrizations for proton–proton cross-sections and asymptotia, *J. Phys. G* 40 (2013) 125001, Erratum: *J. Phys. G* 41 (2014) 019501, arXiv:1305.2947 [hep-ph].
- [26] M.M. Block, R.N. Cahn, High energy predictions for $\bar{p}p$ and pp elastic scattering and total cross sections, *Czechoslov. J. Phys.* 40 (1990) 164.
- [27] A.K. Kohara, E. Ferreira, T. Kodama, Amplitudes and observables in pp elastic scattering at $\sqrt{s} = 7$ TeV, *Eur. Phys. J. C* 73 (2013) 2326, arXiv:1212.3652 [hep-ph].
- [28] O.V. Selyugin, Total cross sections and ρ at high energy, *Nucl. Phys. A* 922 (2014) 180, arXiv:1312.1271 [hep-ph].
- [29] R.J.N. Phillips, V.D. Barger, Model independent analysis of the structure in pp scattering, *Phys. Lett. B* 46 (1973) 412.
- [30] D.A. Fagundes, et al., Elastic pp scattering from the optical point to past the dip: an empirical parametrization from ISR to the LHC, *Phys. Rev. D* 88 (2013) 094019, arXiv:1306.0452 [hep-ph].
- [31] C. Bourrely, J. Soffer, T.T. Wu, Determination of the forward slope in $\bar{p}p$ and $p-p$ elastic scattering up to LHC energy, *Eur. Phys. J. C* 71 (2011) 1601, arXiv:1011.1756 [hep-ph].
- [32] T. Sjostrand, S. Mrenna, P. Skands, A brief introduction to PYTHIA 8.1, *Comput. Phys. Commun.* 178 (2008) 852–867, arXiv:0710.3820 [hep-ph].
- [33] T. Sjostrand, S. Mrenna, P. Skands, PYTHIA 6.4 physics and manual, *J. High Energy Phys.* 05 (2006) 026, arXiv:hep-ph/0603175.
- [34] CERN Accelerator Beam Physics Group, MAD – Methodical Accelerator Design, <http://mad.web.cern.ch/mad/>, 2014.
- [35] R. Ciesielski, K. Goulianos, MBR Monte Carlo simulation in PYTHIA8, in: PoS ICHEP2012, 2013, p. 301, arXiv:1205.1446 [hep-ph].
- [36] B. Malaescu, An Iterative, Dynamically Stabilized (IDS) method of data unfolding, arXiv:1106.3107 [physics.data-an], 2011.
- [37] ATLAS Collaboration, Luminosity determination in pp collisions at $\sqrt{s} = 8$ TeV using the ATLAS detector at the LHC, CERN-EP-2016-117, 2016, arXiv:1608.03953 [hep-ex].
- [38] S. van der Meer, Calibration of the effective beam height in the ISR, *ISR-PO-68-31*, 1968; <http://cds.cern.ch/record/296752>.
- [39] J. Allison, et al., Geant4 developments and applications, *IEEE Trans. Nucl. Sci.* 53 (2006) 270.
- [40] S. Agostinelli, et al., GEANT4 – a simulation toolkit, *Nucl. Instrum. Methods A* 506 (2003) 250.
- [41] V. Blobel, Some comments on χ^2 minimization applications, eConf C030908 (2003) MOET002, <http://www.slac.stanford.edu/econf/C030908/proceedings.html>.
- [42] M.G. Ryskin, A.D. Martin, V.A. Khoze, Soft diffraction and the elastic slope at Tevatron and LHC energies: a multi-Pomeron approach, *Eur. Phys. J. C* 18 (2000) 167, arXiv:hep-ph/0007359.
- [43] J.C. Bernauer, et al., A1 Collaboration, Electric and magnetic form factors of the proton, *Phys. Rev. C* 90 (2014) 015206, arXiv:1307.6227 [nucl-ex].
- [44] P. Abreu, et al., Pierre Auger Collaboration, Measurement of the proton-air cross-section at $\sqrt{s} = 57$ TeV with the Pierre Auger observatory, *Phys. Rev. Lett.* 109 (2012) 062002, arXiv:1208.1520 [hep-ex].
- [45] G. Aielli, et al., ARGO-YBJ Collaboration, Proton–air cross section measurement with the ARGO-YBJ cosmic ray experiment, *Phys. Rev. D* 80 (2009) 092004, arXiv:0904.4198 [hep-ex].
- [46] M. Honda, et al., Inelastic cross-section for p -air collisions from air shower experiments and total cross-section for p - p collisions up to $\sqrt{s} = 24$ TeV, *Phys. Rev. Lett.* 70 (1993) 525.
- [47] R.M. Baltrusaitis, et al., Total proton–proton cross-section at $\sqrt{s} = 30$ TeV, *Phys. Rev. Lett.* 52 (1984) 1380.
- [48] V.A. Schegelsky, M.G. Ryskin, The diffraction cone shrinkage speed up with the collision energy, *Phys. Rev. D* 85 (2012) 094024, arXiv:1112.3243 [hep-ph].
- [49] G. Antchev, et al., TOTEM Collaboration, Evidence for non-exponential elastic proton–proton differential cross-section at low $|t|$ and $\sqrt{s} = 8$ TeV by TOTEM, *Nucl. Phys. B* 899 (2015) 527, arXiv:1503.08111 [hep-ex].
- [50] ATLAS Collaboration, ATLAS Computing Acknowledgements 2016–2017, ATLAS-PUB-2016-002, 2016, <http://cds.cern.ch/record/2202407>.

The ATLAS Collaboration

M. Aaboud^{135d}, G. Aad⁸⁶, B. Abbott¹¹³, J. Abdallah⁶⁴, O. Abdinov¹², B. Abeloos¹¹⁷, R. Aben¹⁰⁷, O.S. AbouZeid¹³⁷, N.L. Abraham¹⁴⁹, H. Abramowicz¹⁵³, H. Abreu¹⁵², R. Abreu¹¹⁶, Y. Abulaiti^{146a,146b}, B.S. Acharya^{163a,163b,a}, S. Adachi¹⁵⁵, L. Adamczyk^{40a}, D.L. Adams²⁷, J. Adelman¹⁰⁸, S. Adomeit¹⁰⁰, T. Adye¹³¹, A.A. Affolder⁷⁵, T. Agatonovic-Jovin¹⁴, J. Agricola⁵⁶, J.A. Aguilar-Saavedra^{126a,126f}, S.P. Ahlen²⁴, F. Ahmadov^{66,b}, G. Aielli^{133a,133b}, H. Akerstedt^{146a,146b}, T.P.A. Åkesson⁸², A.V. Akimov⁹⁶, G.L. Alberghi^{22a,22b}, J. Albert¹⁶⁸, S. Albrand⁵⁷, M.J. Alconada Verzini⁷², M. Aleksa³², I.N. Aleksandrov⁶⁶, C. Alexa^{28b}, G. Alexander¹⁵³, T. Alexopoulos¹⁰, M. Alhroob¹¹³, B. Ali¹²⁸, M. Aliev^{74a,74b}, G. Alimonti^{92a}, J. Alison³³, S.P. Alkire³⁷, B.M.M. Allbrooke¹⁴⁹, B.W. Allen¹¹⁶, P.P. Allport¹⁹, A. Aloisio^{104a,104b}, A. Alonso³⁸, F. Alonso⁷², C. Alpigiani¹³⁸, A.A. Alshehri⁵⁵, M. Alstamy⁸⁶, B. Alvarez Gonzalez³², D. Álvarez Piqueras¹⁶⁶, M.G. Alviggi^{104a,104b}, B.T. Amadio¹⁶, K. Amako⁶⁷, Y. Amaral Coutinho^{26a}, C. Amelung²⁵, D. Amidei⁹⁰, S.P. Amor Dos Santos^{126a,126c}, A. Amorim^{126a,126b}, S. Amoroso³², G. Amundsen²⁵, C. Anastopoulos¹³⁹, L.S. Ancu⁵¹, N. Andari¹⁹, T. Andeen¹¹, C.F. Anders^{59b}, G. Anders³², J.K. Anders⁷⁵, K.J. Anderson³³, A. Andreazza^{92a,92b}, V. Andrei^{59a}, S. Angelidakis⁹, I. Angelozzi¹⁰⁷, P. Anger⁴⁶, A. Angerami³⁷, F. Anghinolfi³², A.V. Anisenkov^{109,c}, N. Anjos¹³, A. Annovi^{124a,124b}, C. Antel^{59a}, M. Antonelli⁴⁹, A. Antonov^{98,*}, F. Anulli^{132a}, M. Aoki⁶⁷, L. Aperio Bella¹⁹, G. Arabidze⁹¹, Y. Arai⁶⁷, J.P. Araque^{126a}, A.T.H. Arce⁴⁷, F.A. Arduh⁷², J-F. Arguin⁹⁵, S. Argyropoulos⁶⁴, M. Arik^{20a}, A.J. Armbruster¹⁴³, L.J. Armitage⁷⁷, O. Arnaez³², H. Arnold⁵⁰, M. Arratia³⁰, O. Arslan²³, A. Artamonov⁹⁷, G. Artoni¹²⁰, S. Artz⁸⁴, S. Asai¹⁵⁵, N. Asbah⁴⁴, A. Ashkenazi¹⁵³, B. Åsman^{146a,146b},

L. Asquith¹⁴⁹, K. Assamagan²⁷, R. Astalos^{144a}, M. Atkinson¹⁶⁵, N.B. Atlay¹⁴¹, K. Augsten¹²⁸, G. Avolio³², B. Axen¹⁶, M.K. Ayoub¹¹⁷, G. Azuelos^{95,d}, M.A. Baak³², A.E. Baas^{59a}, M.J. Baca¹⁹, H. Bachacou¹³⁶, K. Bachas^{74a,74b}, M. Backes¹²⁰, M. Backhaus³², P. Bagiacci^{132a,132b}, P. Bagnaia^{132a,132b}, Y. Bai^{35a}, J.T. Baines¹³¹, O.K. Baker¹⁷⁵, E.M. Baldin^{109,c}, P. Balek¹⁷¹, T. Balestri¹⁴⁸, F. Balli¹³⁶, W.K. Balunas¹²², E. Banas⁴¹, Sw. Banerjee^{172,e}, A.A.E. Bannoura¹⁷⁴, L. Barak³², E.L. Barberio⁸⁹, D. Barberis^{52a,52b}, M. Barbero⁸⁶, T. Barillari¹⁰¹, M-S Barisits³², T. Barklow¹⁴³, N. Barlow³⁰, S.L. Barnes⁸⁵, B.M. Barnett¹³¹, R.M. Barnett¹⁶, Z. Barnovska-Blenessy⁵, A. Baroncelli^{134a}, G. Barone²⁵, A.J. Barr¹²⁰, L. Barranco Navarro¹⁶⁶, F. Barreiro⁸³, J. Barreiro Guimarães da Costa^{35a}, R. Bartoldus¹⁴³, A.E. Barton⁷³, P. Bartos^{144a}, A. Basalae¹²³, A. Bassalat¹¹⁷, R.L. Bates⁵⁵, S.J. Batista¹⁵⁸, J.R. Batley³⁰, M. Battaglia¹³⁷, M. Bauce^{132a,132b}, F. Bauer¹³⁶, H.S. Bawa^{143,f}, J.B. Beacham¹¹¹, M.D. Beattie⁷³, T. Beau⁸¹, P.H. Beauchemin¹⁶¹, P. Bechtel²³, H.P. Beck^{18,g}, K. Becker¹²⁰, M. Becker⁸⁴, M. Beckingham¹⁶⁹, C. Becot¹¹⁰, A.J. Beddall^{20e}, A. Beddall^{20b}, V.A. Bednyakov⁶⁶, M. Bedognetti¹⁰⁷, C.P. Bee¹⁴⁸, L.J. Beemster¹⁰⁷, T.A. Beermann³², M. Begel²⁷, J.K. Behr⁴⁴, C. Belanger-Champagne⁸⁸, A.S. Bell⁷⁹, G. Bella¹⁵³, L. Bellagamba^{22a}, A. Bellerive³¹, M. Bellomo⁸⁷, K. Belotskiy⁹⁸, O. Beltramello³², N.L. Belyaev⁹⁸, O. Benary¹⁵³, D. Benchekroun^{135a}, M. Bender¹⁰⁰, K. Bendtz^{146a,146b}, N. Benekos¹⁰, Y. Benhammou¹⁵³, E. Benhar Noccioli¹⁷⁵, J. Benitez⁶⁴, D.P. Benjamin⁴⁷, J.R. Bensinger²⁵, S. Bentvelsen¹⁰⁷, L. Beresford¹²⁰, M. Beretta⁴⁹, D. Berge¹⁰⁷, E. Bergeas Kuutmann¹⁶⁴, N. Berger⁵, J. Beringer¹⁶, S. Berlendis⁵⁷, N.R. Bernard⁸⁷, C. Bernius¹¹⁰, F.U. Bernlochner²³, T. Berry⁷⁸, P. Berta¹²⁹, C. Bertella⁸⁴, G. Bertoli^{146a,146b}, F. Bertolucci^{124a,124b}, I.A. Bertram⁷³, C. Bertsche⁴⁴, D. Bertsche¹¹³, G.J. Besjes³⁸, O. Bessidskaia Bylund^{146a,146b}, M. Bessner⁴⁴, N. Besson¹³⁶, C. Betancourt⁵⁰, A. Bethani⁵⁷, S. Bethke¹⁰¹, A.J. Bevan⁷⁷, R.M. Bianchi¹²⁵, L. Bianchini²⁵, M. Bianco³², O. Biebel¹⁰⁰, D. Biedermann¹⁷, R. Bielski⁸⁵, N.V. Biesuz^{124a,124b}, M. Biglietti^{134a}, J. Bilbao De Mendizabal⁵¹, T.R.V. Billoud⁹⁵, H. Bilokon⁴⁹, M. Bindi⁵⁶, S. Binet¹¹⁷, A. Bingul^{20b}, C. Bini^{132a,132b}, S. Biondi^{22a,22b}, T. Bisanz⁵⁶, D.M. Bjergaard⁴⁷, C.W. Black¹⁵⁰, J.E. Black¹⁴³, K.M. Black²⁴, D. Blackburn¹³⁸, R.E. Blair⁶, J.-B. Blanchard¹³⁶, T. Blazek^{144a}, I. Bloch⁴⁴, C. Blocker²⁵, A. Blue⁵⁵, W. Blum^{84,*}, U. Blumenschein⁵⁶, S. Blunier^{34a}, G.J. Bobbink¹⁰⁷, V.S. Bobrovnikov^{109,c}, S.S. Bocchetta⁸², A. Bocci⁴⁷, C. Bock¹⁰⁰, M. Boehler⁵⁰, D. Boerner¹⁷⁴, J.A. Bogaerts³², D. Bogavac¹⁴, A.G. Bogdanchikov¹⁰⁹, C. Bohm^{146a}, V. Boisvert⁷⁸, P. Bokan¹⁴, T. Bold^{40a}, A.S. Boldyrev^{163a,163c}, M. Bomben⁸¹, M. Bona⁷⁷, M. Boonekamp¹³⁶, A. Borisov¹³⁰, G. Borissov⁷³, J. Bortfeldt³², D. Bortoletto¹²⁰, V. Bortolotto^{61a,61b,61c}, K. Bos¹⁰⁷, D. Boscherini^{22a}, M. Bosman¹³, J.D. Bossio Sola²⁹, J. Boudreau¹²⁵, J. Bouffard², E.V. Bouhova-Thacker⁷³, D. Boumediene³⁶, C. Bourdarios¹¹⁷, S.K. Boutle⁵⁵, A. Boveia³², J. Boyd³², I.R. Boyko⁶⁶, J. Bracinik¹⁹, A. Brandt⁸, G. Brandt⁵⁶, O. Brandt^{59a}, U. Bratzler¹⁵⁶, B. Brau⁸⁷, J.E. Brau¹¹⁶, W.D. Breaden Madden⁵⁵, K. Brendlinger¹²², A.J. Brennan⁸⁹, L. Brenner¹⁰⁷, R. Brenner¹⁶⁴, S. Bressler¹⁷¹, T.M. Bristow⁴⁸, D. Britton⁵⁵, D. Britzger⁴⁴, F.M. Brochu³⁰, I. Brock²³, R. Brock⁹¹, G. Brooijmans³⁷, T. Brooks⁷⁸, W.K. Brooks^{34b}, J. Brosamer¹⁶, E. Brost¹⁰⁸, J.H. Broughton¹⁹, P.A. Bruckman de Renstrom⁴¹, D. Bruncko^{144b}, R. Bruneliere⁵⁰, A. Bruni^{22a}, G. Bruni^{22a}, L.S. Bruni¹⁰⁷, B.H. Brunt³⁰, M. Bruschi^{22a}, N. Bruscino²³, P. Bryant³³, L. Bryngemark⁸², T. Buanes¹⁵, Q. Buat¹⁴², P. Buchholz¹⁴¹, A.G. Buckley⁵⁵, I.A. Budagov⁶⁶, F. Buehrer⁵⁰, M.K. Bugge¹¹⁹, O. Bulekov⁹⁸, D. Bullock⁸, H. Burckhart³², S. Burdin⁷⁵, C.D. Burgard⁵⁰, B. Burghgrave¹⁰⁸, K. Burka⁴¹, S. Burke¹³¹, I. Burmeister⁴⁵, J.T.P. Burr¹²⁰, E. Busato³⁶, D. Büscher⁵⁰, V. Büscher⁸⁴, P. Bussey⁵⁵, J.M. Butler²⁴, C.M. Buttar⁵⁵, J.M. Butterworth⁷⁹, P. Butti¹⁰⁷, W. Buttinger²⁷, A. Buzatu⁵⁵, A.R. Buzykaev^{109,c}, G. Cabras^{22a,22b}, S. Cabrera Urbán¹⁶⁶, D. Caforio¹²⁸, V.M. Cairo^{39a,39b}, O. Cakir^{4a}, N. Calace⁵¹, P. Calafiura¹⁶, A. Calandri⁸⁶, G. Calderini⁸¹, P. Calfayan¹⁰⁰, G. Callea^{39a,39b}, L.P. Caloba^{26a}, S. Calvente Lopez⁸³, D. Calvet³⁶, S. Calvet³⁶, T.P. Calvet⁸⁶, R. Camacho Toro³³, S. Camarda³², P. Camarri^{133a,133b}, D. Cameron¹¹⁹, R. Caminal Armadans¹⁶⁵, C. Camincher⁵⁷, S. Campana³², M. Campanelli⁷⁹, A. Camplani^{92a,92b}, A. Campoverde¹⁴¹, V. Canale^{104a,104b}, A. Canepa^{159a}, M. Cano Bret^{35e}, J. Cantero¹¹⁴, T. Cao⁴², M.D.M. Capeans Garrido³², I. Caprini^{28b}, M. Caprini^{28b}, M. Capua^{39a,39b}, R.M. Carbone³⁷, R. Cardarelli^{133a}, F. Cardillo⁵⁰, I. Carli¹²⁹, T. Carli³², G. Carlino^{104a}, L. Carminati^{92a,92b}, S. Caron¹⁰⁶, E. Carquin^{34b}, G.D. Carrillo-Montoya³², J.R. Carter³⁰, J. Carvalho^{126a,126c}, D. Casadei¹⁹, M.P. Casado^{13,h}, M. Casolino¹³, D.W. Casper¹⁶², E. Castaneda-Miranda^{145a}, R. Castelijns¹⁰⁷, A. Castelli¹⁰⁷, V. Castillo Gimenez¹⁶⁶, N.F. Castro^{126a,i}, A. Catinaccio³², J.R. Catmore¹¹⁹, A. Cattai³², J. Caudron²³, V. Cavaliere¹⁶⁵, E. Cavallaro¹³, D. Cavalli^{92a}, M. Cavalli-Sforza¹³, V. Cavasinni^{124a,124b}, F. Ceradini^{134a,134b}, L. Cerda Alberich¹⁶⁶, B.C. Cerio⁴⁷,

A.S. Cerqueira^{26b}, A. Cerri¹⁴⁹, L. Cerrito^{133a,133b}, F. Cerutti¹⁶, M. Cerv³², A. Cervelli¹⁸, S.A. Cetin^{20d},
 A. Chafaq^{135a}, D. Chakraborty¹⁰⁸, S.K. Chan⁵⁸, Y.L. Chan^{61a}, P. Chang¹⁶⁵, J.D. Chapman³⁰,
 D.G. Charlton¹⁹, A. Chatterjee⁵¹, C.C. Chau¹⁵⁸, C.A. Chavez Barajas¹⁴⁹, S. Che¹¹¹, S. Cheatham^{163a,163c},
 A. Chegwidden⁹¹, S. Chekanov⁶, S.V. Chekulaev^{159a}, G.A. Chelkov^{66,j}, M.A. Chelstowska⁹⁰, C. Chen⁶⁵,
 H. Chen²⁷, K. Chen¹⁴⁸, S. Chen^{35c}, S. Chen¹⁵⁵, X. Chen^{35f}, Y. Chen⁶⁸, H.C. Cheng⁹⁰, H.J. Cheng^{35a},
 Y. Cheng³³, A. Cheplakov⁶⁶, E. Cheremushkina¹³⁰, R. Cherkaoui El Moursli^{135e}, V. Chernyatin^{27,*},
 E. Cheu⁷, L. Chevalier¹³⁶, V. Chiarella⁴⁹, G. Chiarelli^{124a,124b}, G. Chiodini^{74a}, A.S. Chisholm³²,
 A. Chitan^{28b}, M.V. Chizhov⁶⁶, K. Choi⁶², A.R. Chomont³⁶, S. Chouridou⁹, B.K.B. Chow¹⁰⁰,
 V. Christodoulou⁷⁹, D. Chromek-Burckhart³², J. Chudoba¹²⁷, A.J. Chuinard⁸⁸, J.J. Chwastowski⁴¹,
 L. Chytka¹¹⁵, G. Ciapetti^{132a,132b}, A.K. Ciftci^{4a}, D. Cinca⁴⁵, V. Cindro⁷⁶, I.A. Cioara²³, C. Ciocca^{22a,22b},
 A. Ciochio¹⁶, F. Ciotto^{104a,104b}, Z.H. Citron¹⁷¹, M. Citterio^{92a}, M. Ciubancan^{28b}, A. Clark⁵¹, B.L. Clark⁵⁸,
 M.R. Clark³⁷, P.J. Clark⁴⁸, R.N. Clarke¹⁶, C. Clement^{146a,146b}, Y. Coadou⁸⁶, M. Cokal^{163a,163c},
 A. Coccaro⁵¹, J. Cochran⁶⁵, L. Colasurdo¹⁰⁶, B. Cole³⁷, A.P. Colijn¹⁰⁷, J. Collot⁵⁷, T. Colombo¹⁶²,
 G. Compostella¹⁰¹, P. Conde Muño^{126a,126b}, E. Coniavitis⁵⁰, S.H. Connell^{145b}, I.A. Connelly⁷⁸,
 V. Consorti⁵⁰, S. Constantinescu^{28b}, G. Conti³², F. Conventi^{104a,k}, M. Cooke¹⁶, B.D. Cooper⁷⁹,
 A.M. Cooper-Sarkar¹²⁰, K.J.R. Cormier¹⁵⁸, T. Cornelissen¹⁷⁴, M. Corradi^{132a,132b}, F. Corriveau^{88,l},
 A. Corso-Radu¹⁶², A. Cortes-Gonzalez³², G. Cortiana¹⁰¹, G. Costa^{92a}, M.J. Costa¹⁶⁶, D. Costanzo¹³⁹,
 G. Cottin³⁰, G. Cowan⁷⁸, B.E. Cox⁸⁵, K. Cranmer¹¹⁰, S.J. Crawley⁵⁵, G. Cree³¹, S. Crépé-Renaudin⁵⁷,
 F. Crescioli⁸¹, W.A. Cribbs^{146a,146b}, M. Crispin Ortuzar¹²⁰, M. Cristinziani²³, V. Croft¹⁰⁶,
 G. Crosetti^{39a,39b}, A. Cueto⁸³, T. Cuhadar Donszelmann¹³⁹, J. Cummings¹⁷⁵, M. Curatolo⁴⁹, J. Cúth⁸⁴,
 H. Czirr¹⁴¹, P. Czodrowski³, G. D'amen^{22a,22b}, S. D'Auria⁵⁵, M. D'Onofrio⁷⁵,
 M.J. Da Cunha Sargedas De Sousa^{126a,126b}, C. Da Via⁸⁵, W. Dabrowski^{40a}, T. Dado^{144a}, T. Dai⁹⁰,
 O. Dale¹⁵, F. Dallaire⁹⁵, C. Dallapiccola⁸⁷, M. Dam³⁸, J.R. Dandoy³³, N.P. Dang⁵⁰, A.C. Daniells¹⁹,
 N.S. Dann⁸⁵, M. Danninger¹⁶⁷, M. Dano Hoffmann¹³⁶, V. Dao⁵⁰, G. Darbo^{52a}, S. Darmora⁸,
 J. Dassoulas³, A. Dattagupta⁶², W. Davey²³, C. David¹⁶⁸, T. Davidek¹²⁹, M. Davies¹⁵³, P. Davison⁷⁹,
 E. Dawe⁸⁹, I. Dawson¹³⁹, K. De⁸, R. de Asmundis^{104a}, A. De Benedetti¹¹³, S. De Castro^{22a,22b},
 S. De Cecco⁸¹, N. De Groot¹⁰⁶, P. de Jong¹⁰⁷, H. De la Torre⁹¹, F. De Lorenzi⁶⁵, A. De Maria⁵⁶,
 D. De Pedis^{132a}, A. De Salvo^{132a}, U. De Sanctis¹⁴⁹, A. De Santo¹⁴⁹, J.B. De Vivie De Regie¹¹⁷,
 W.J. Dearnaley⁷³, R. Debbé²⁷, C. Debenedetti¹³⁷, D.V. Dedovich⁶⁶, N. Dehghanian³, I. Deigaard¹⁰⁷,
 M. Del Gaudio^{39a,39b}, J. Del Peso⁸³, T. Del Prete^{124a,124b}, D. Delgove¹¹⁷, F. Deliot¹³⁶, C.M. Delitzsch⁵¹,
 A. Dell'Acqua³², L. Dell'Asta²⁴, M. Dell'Orso^{124a,124b}, M. Della Pietra^{104a,k}, D. della Volpe⁵¹,
 M. Delmastro⁵, P.A. Delsart⁵⁷, D.A. DeMarco¹⁵⁸, S. Demers¹⁷⁵, M. Demichev⁶⁶, A. Demilly⁸¹,
 S.P. Denisov¹³⁰, D. Denysiuk¹³⁶, D. Derendarz⁴¹, J.E. Derkaoui^{135d}, F. Derue⁸¹, P. Dervan⁷⁵, K. Desch²³,
 C. Deterre⁴⁴, K. Dette⁴⁵, P.O. Deviveiros³², A. Dewhurst¹³¹, S. Dhaliwal²⁵, A. Di Ciaccio^{133a,133b},
 L. Di Ciaccio⁵, W.K. Di Clemente¹²², C. Di Donato^{132a,132b}, A. Di Girolamo³², B. Di Girolamo³²,
 B. Di Micco^{134a,134b}, R. Di Nardo³², A. Di Simone⁵⁰, R. Di Sipio¹⁵⁸, D. Di Valentino³¹, C. Diaconu⁸⁶,
 M. Diamond¹⁵⁸, F.A. Dias⁴⁸, M.A. Diaz^{34a}, E.B. Diehl⁹⁰, J. Dietrich¹⁷, S. Díez Cornell⁴⁴,
 A. Dimitrievska¹⁴, J. Dingfelder²³, P. Dita^{28b}, S. Dita^{28b}, F. Dittus³², F. Djama⁸⁶, T. Djobava^{53b},
 J.I. Djuvsland^{59a}, M.A.B. do Vale^{26c}, D. Dobos³², M. Dobre^{28b}, C. Doglioni⁸², J. Dolejsi¹²⁹, Z. Dolezal¹²⁹,
 M. Donadelli^{26d}, S. Donati^{124a,124b}, P. Dondero^{121a,121b}, J. Donini³⁶, J. Dopke¹³¹, A. Doria^{104a},
 M.T. Dova⁷², A.T. Doyle⁵⁵, E. Drechsler⁵⁶, M. Dris¹⁰, Y. Du^{35d}, J. Duarte-Campderros¹⁵³, E. Duchovni¹⁷¹,
 G. Duckeck¹⁰⁰, O.A. Ducu^{95,m}, D. Duda¹⁰⁷, A. Dudarev³², A.Ch. Dudder⁸⁴, E.M. Duffield¹⁶, L. Duflo¹¹⁷,
 M. Dührssen³², M. Dumancic¹⁷¹, M. Dunford^{59a}, H. Duran Yildiz^{4a}, M. Düren⁵⁴, A. Durglishvili^{53b},
 D. Duschinger⁴⁶, B. Dutta⁴⁴, M. Dyndal⁴⁴, C. Eckardt⁴⁴, K.M. Ecker¹⁰¹, R.C. Edgar⁹⁰, N.C. Edwards⁴⁸,
 T. Eifert³², G. Eigen¹⁵, K. Einsweiler¹⁶, T. Ekelof¹⁶⁴, M. El Kacimi^{135c}, V. Ellajosyula⁸⁶, M. Ellert¹⁶⁴,
 S. Elles⁵, F. Ellinghaus¹⁷⁴, A.A. Elliot¹⁶⁸, N. Ellis³², J. Elmsheuser²⁷, M. Elsing³², D. Emeliyanov¹³¹,
 Y. Enari¹⁵⁵, O.C. Endner⁸⁴, J.S. Ennis¹⁶⁹, J. Erdmann⁴⁵, A. Ereditato¹⁸, G. Ernis¹⁷⁴, J. Ernst², M. Ernst²⁷,
 S. Errede¹⁶⁵, E. Ertel⁸⁴, M. Escalier¹¹⁷, H. Esch⁴⁵, C. Escobar¹²⁵, B. Esposito⁴⁹, A.I. Etienvre¹³⁶,
 E. Etzion¹⁵³, H. Evans⁶², A. Ezhilov¹²³, M. Ezzi^{135e}, F. Fabbri^{22a,22b}, L. Fabbri^{22a,22b}, G. Facini³³,
 R.M. Fakhruddinov¹³⁰, S. Falciano^{132a}, R.J. Falla⁷⁹, J. Faltova³², Y. Fang^{35a}, M. Fanti^{92a,92b}, A. Farbin⁸,
 A. Farilla^{134a}, C. Farina¹²⁵, E.M. Farina^{121a,121b}, T. Farooque¹³, S. Farrell¹⁶, S.M. Farrington¹⁶⁹,
 P. Farthouat³², F. Fassi^{135e}, P. Fassnacht³², D. Fassoulotis⁹, M. Fauci Giannelli⁷⁸, A. Favareto^{52a,52b},

W.J. Fawcett¹²⁰, L. Fayard¹¹⁷, O.L. Fedin^{123,n}, W. Fedorko¹⁶⁷, S. Feigl¹¹⁹, L. Feligioni⁸⁶, C. Feng^{35d}, E.J. Feng³², H. Feng⁹⁰, A.B. Fenyuk¹³⁰, L. Feremenga⁸, P. Fernandez Martinez¹⁶⁶, S. Fernandez Perez¹³, J. Ferrando⁴⁴, A. Ferrari¹⁶⁴, P. Ferrari¹⁰⁷, R. Ferrari^{121a}, D.E. Ferreira de Lima^{59b}, A. Ferrer¹⁶⁶, D. Ferrere⁵¹, C. Ferretti⁹⁰, A. Ferretto Parodi^{52a,52b}, F. Fiedler⁸⁴, A. Filipčič⁷⁶, M. Filipuzzi⁴⁴, F. Filthaut¹⁰⁶, M. Fincke-Keeler¹⁶⁸, K.D. Finelli¹⁵⁰, M.C.N. Fiolhais^{126a,126c}, L. Fiorini¹⁶⁶, A. Firan⁴², A. Fischer², C. Fischer¹³, J. Fischer¹⁷⁴, W.C. Fisher⁹¹, N. Flaschel⁴⁴, I. Fleck¹⁴¹, P. Fleischmann⁹⁰, G.T. Fletcher¹³⁹, R.R.M. Fletcher¹²², T. Flick¹⁷⁴, L.R. Flores Castillo^{61a}, M.J. Flowerdew¹⁰¹, G.T. Forcolin⁸⁵, A. Formica¹³⁶, A. Forti⁸⁵, A.G. Foster¹⁹, D. Fournier¹¹⁷, H. Fox⁷³, S. Fracchia¹³, P. Francavilla⁸¹, M. Franchini^{22a,22b}, D. Francis³², L. Franconi¹¹⁹, M. Franklin⁵⁸, M. Frate¹⁶², M. Fraternali^{121a,121b}, D. Freeborn⁷⁹, S.M. Fressard-Batraneanu³², F. Friedrich⁴⁶, D. Froidevaux³², J.A. Frost¹²⁰, C. Fukunaga¹⁵⁶, E. Fullana Torregrosa⁸⁴, T. Fusayasu¹⁰², J. Fuster¹⁶⁶, C. Gabaldon⁵⁷, O. Gabizon¹⁷⁴, A. Gabrielli^{22a,22b}, A. Gabrielli¹⁶, G.P. Gach^{40a}, S. Gadatsch³², S. Gadomski⁷⁸, G. Gagliardi^{52a,52b}, L.G. Gagnon⁹⁵, P. Gagnon⁶², C. Galea¹⁰⁶, B. Galhardo^{126a,126c}, E.J. Gallas¹²⁰, B.J. Gallop¹³¹, P. Gallus¹²⁸, G. Galster³⁸, K.K. Gan¹¹¹, J. Gao^{35b}, Y. Gao⁴⁸, Y.S. Gao^{143,f}, F.M. Garay Walls⁴⁸, C. García¹⁶⁶, J.E. García Navarro¹⁶⁶, M. Garcia-Sciveres¹⁶, R.W. Gardner³³, N. Garelli¹⁴³, V. Garonne¹¹⁹, A. Gascon Bravo⁴⁴, K. Gasnikova⁴⁴, C. Gatti⁴⁹, A. Gaudiello^{52a,52b}, G. Gaudio^{121a}, L. Gauthier⁹⁵, I.L. Gavrilenko⁹⁶, C. Gay¹⁶⁷, G. Gaycken²³, E.N. Gazis¹⁰, Z. Gece¹⁶⁷, C.N.P. Gee¹³¹, Ch. Geich-Gimbel²³, M. Geisen⁸⁴, M.P. Geisler^{59a}, K. Gellerstedt^{146a,146b}, C. Gemme^{52a}, M.H. Genest⁵⁷, C. Geng^{35b,o}, S. Gentile^{132a,132b}, C. Gentsos¹⁵⁴, S. George⁷⁸, D. Gerbaudo¹³, A. Gershon¹⁵³, S. Ghasemi¹⁴¹, M. Ghneimat²³, B. Giacobbe^{22a}, S. Giagu^{132a,132b}, P. Giannetti^{124a,124b}, B. Gibbard²⁷, S.M. Gibson⁷⁸, M. Gignac¹⁶⁷, M. Gilchriese¹⁶, T.P.S. Gillam³⁰, D. Gillberg³¹, G. Gilles¹⁷⁴, D.M. Gingrich^{3,d}, N. Giokaris⁹, M.P. Giordani^{163a,163c}, F.M. Giorgi^{22a}, F.M. Giorgi¹⁷, P.F. Giraud¹³⁶, P. Giromini⁵⁸, D. Giugni^{92a}, F. Giuli¹²⁰, C. Giuliani¹⁰¹, M. Giulini^{59b}, B.K. Gjelsten¹¹⁹, S. Gkaitatzis¹⁵⁴, I. Gkialas¹⁵⁴, E.L. Gkougkousis¹¹⁷, L.K. Gladilin⁹⁹, C. Glasman⁸³, J. Glatzer⁵⁰, P.C.F. Glaysher⁴⁸, A. Glazov⁴⁴, M. Goblirsch-Kolb²⁵, J. Godlewski⁴¹, S. Goldfarb⁸⁹, T. Golling⁵¹, D. Golubkov¹³⁰, A. Gomes^{126a,126b,126d}, R. Gonçalo^{126a}, J. Goncalves Pinto Firmino Da Costa¹³⁶, G. Gonella⁵⁰, L. Gonella¹⁹, A. Gongadze⁶⁶, S. González de la Hoz¹⁶⁶, G. Gonzalez Parra¹³, S. Gonzalez-Sevilla⁵¹, L. Goossens³², P.A. Gorbounov⁹⁷, H.A. Gordon²⁷, I. Gorelov¹⁰⁵, B. Gorini³², E. Gorini^{74a,74b}, A. Gorišek⁷⁶, E. Gornicki⁴¹, A.T. Goshaw⁴⁷, C. Gössling⁴⁵, M.I. Gostkin⁶⁶, C.R. Goudet¹¹⁷, D. Goujdami^{135c}, A.G. Goussiou¹³⁸, N. Govender^{145b,p}, E. Gozani¹⁵², L. Graber⁵⁶, I. Grabowska-Bold^{40a}, P.O.J. Gradin⁵⁷, P. Grafström^{22a,22b}, J. Gramling⁵¹, E. Gramstad¹¹⁹, S. Grancagnolo¹⁷, V. Gratchev¹²³, P.M. Gravila^{28e}, H.M. Gray³², E. Graziani^{134a}, Z.D. Greenwood^{80,q}, C. Grefe²³, K. Gregersen⁷⁹, I.M. Gregor⁴⁴, P. Grenier¹⁴³, K. Grevtsov⁵, J. Griffiths⁸, A.A. Grillo¹³⁷, K. Grimm⁷³, S. Grinstein^{13,r}, Ph. Gris³⁶, J.-F. Grivaz¹¹⁷, S. Groh⁸⁴, J.P. Grohs⁴⁶, E. Gross¹⁷¹, J. Grosse-Knetter⁵⁶, G.C. Grossi⁸⁰, Z.J. Grout⁷⁹, L. Guan⁹⁰, W. Guan¹⁷², J. Guenther⁶³, F. Guescini⁵¹, D. Guest¹⁶², O. Gueta¹⁵³, E. Guido^{52a,52b}, T. Guillemin⁵, S. Guindon², U. Gul⁵⁵, C. Gumpert³², J. Guo^{35e}, Y. Guo^{35b,o}, R. Gupta⁴², S. Gupta¹²⁰, G. Gustavino^{132a,132b}, P. Gutierrez¹¹³, N.G. Gutierrez Ortiz⁷⁹, C. Gutsche⁴⁶, C. Guyot¹³⁶, C. Gwenlan¹²⁰, C.B. Gwilliam⁷⁵, A. Haas¹¹⁰, C. Haber¹⁶, H.K. Hadavand⁸, N. Haddad^{135e}, A. Hadeef⁸⁶, S. Hageböck²³, M. Hagihara¹⁶⁰, Z. Hajduk⁴¹, H. Hakobyan^{176,*}, M. Haleem⁴⁴, J. Haley¹¹⁴, G. Halladjian⁹¹, G.D. Hallewell⁸⁶, K. Hamacher¹⁷⁴, P. Hamal¹¹⁵, K. Hamano¹⁶⁸, A. Hamilton^{145a}, G.N. Hamity¹³⁹, P.G. Hamnett⁴⁴, L. Han^{35b}, K. Hanagaki^{67,s}, K. Hanawa¹⁵⁵, M. Hance¹³⁷, B. Haney¹²², P. Hanke^{59a}, R. Hanna¹³⁶, J.B. Hansen³⁸, J.D. Hansen³⁸, M.C. Hansen²³, P.H. Hansen³⁸, K. Hara¹⁶⁰, A.S. Hard¹⁷², T. Harenberg¹⁷⁴, F. Hariri¹¹⁷, S. Harkusha⁹³, R.D. Harrington⁴⁸, P.F. Harrison¹⁶⁹, F. Hartjes¹⁰⁷, N.M. Hartmann¹⁰⁰, M. Hasegawa⁶⁸, Y. Hasegawa¹⁴⁰, A. Hasib¹¹³, S. Hassani¹³⁶, S. Haug¹⁸, R. Hauser⁹¹, L. Hauswald⁴⁶, M. Havranek¹²⁷, C.M. Hawkes¹⁹, R.J. Hawking³², D. Hayakawa¹⁵⁷, D. Hayden⁹¹, C.P. Hays¹²⁰, J.M. Hays⁷⁷, H.S. Hayward⁷⁵, S.J. Haywood¹³¹, S.J. Head¹⁹, T. Heck⁸⁴, V. Hedberg⁸², L. Heelan⁸, S. Heim¹²², T. Heim¹⁶, B. Heinemann¹⁶, J.J. Heinrich¹⁰⁰, L. Heinrich¹¹⁰, C. Heinz⁵⁴, J. Hejbal¹²⁷, L. Helary³², S. Hellman^{146a,146b}, C. Hensens³², J. Henderson¹²⁰, R.C.W. Henderson⁷³, Y. Heng¹⁷², S. Henkelmann¹⁶⁷, A.M. Henriques Correia³², S. Henrot-Versille¹¹⁷, G.H. Herbert¹⁷, H. Herde²⁵, V. Herget¹⁷³, Y. Hernández Jiménez¹⁶⁶, G. Herten⁵⁰, R. Hertenberger¹⁰⁰, L. Hervas³², G.G. Hesketh⁷⁹, N.P. Hessey¹⁰⁷, J.W. Hetherly⁴², R. Hickling⁷⁷, E. Higón-Rodríguez¹⁶⁶, E. Hill¹⁶⁸, J.C. Hill³⁰, K.H. Hiller⁴⁴, S.J. Hillier¹⁹, I. Hinchliffe¹⁶, E. Hines¹²², R.R. Hinman¹⁶, M. Hirose⁵⁰, D. Hirschbuehl¹⁷⁴, J. Hobbs¹⁴⁸, N. Hod^{159a},

M.C. Hodgkinson¹³⁹, P. Hodgson¹³⁹, A. Hoecker³², M.R. Hoferkamp¹⁰⁵, F. Hoenig¹⁰⁰, D. Hohn²³, T.R. Holmes¹⁶, M. Homann⁴⁵, T. Honda⁶⁷, T.M. Hong¹²⁵, B.H. Hooberman¹⁶⁵, W.H. Hopkins¹¹⁶, Y. Horii¹⁰³, A.J. Horton¹⁴², J.-Y. Hostachy⁵⁷, S. Hou¹⁵¹, A. Hoummada^{135a}, J. Howarth⁴⁴, J. Hoya⁷², M. Hrabovsky¹¹⁵, I. Hristova¹⁷, J. Hrivnac¹¹⁷, T. Hryn'ova⁵, A. Hrynevich⁹⁴, C. Hsu^{145c}, P.J. Hsu^{151,t}, S.-C. Hsu¹³⁸, Q. Hu^{35b}, S. Hu^{35e}, Y. Huang⁴⁴, Z. Hubacek¹²⁸, F. Hubaut⁸⁶, F. Huegging²³, T.B. Huffman¹²⁰, E.W. Hughes³⁷, G. Hughes⁷³, M. Huhtinen³², P. Huo¹⁴⁸, N. Huseynov^{66,b}, J. Huston⁹¹, J. Huth⁵⁸, G. Iacobucci⁵¹, G. Iakovidis²⁷, I. Ibragimov¹⁴¹, L. Iconomidou-Fayard¹¹⁷, E. Ideal¹⁷⁵, Z. Idrissi^{135e}, P. Iengo³², O. Igonkina^{107,u}, T. Iizawa¹⁷⁰, Y. Ikegami⁶⁷, M. Ikeno⁶⁷, Y. Ilchenko^{11,v}, D. Iliadis¹⁵⁴, N. Ilic¹⁴³, T. Ince¹⁰¹, G. Introzzi^{121a,121b}, P. Ioannou^{9,*}, M. Iodice^{134a}, K. Iordanidou³⁷, V. Ippolito⁵⁸, N. Ishijima¹¹⁸, M. Ishino¹⁵⁵, M. Ishitsuka¹⁵⁷, R. Ishmukhametov¹¹¹, C. Issever¹²⁰, S. Istin^{20a}, F. Ito¹⁶⁰, J.M. Iturbe Ponce⁸⁵, R. Iuppa^{133a,133b}, W. Iwanski⁶³, H. Iwasaki⁶⁷, J.M. Izen⁴³, V. Izzo^{104a}, S. Jabbar³, B. Jackson¹²², P. Jackson¹, V. Jain², K.B. Jakobi⁸⁴, K. Jakobs⁵⁰, S. Jakobsen³², T. Jakoubek¹²⁷, D.O. Jamin¹¹⁴, D.K. Jana⁸⁰, R. Jansky⁶³, J. Janssen²³, M. Janus⁵⁶, G. Jarlskog⁸², N. Javadov^{66,b}, T. Javurek⁵⁰, F. Jeanneau¹³⁶, L. Jeanty¹⁶, G.-Y. Jeng¹⁵⁰, D. Jennens⁸⁹, P. Jenni^{50,w}, C. Jeske¹⁶⁹, S. Jézéquel⁵, H. Ji¹⁷², J. Jia¹⁴⁸, H. Jiang⁶⁵, Y. Jiang^{35b}, S. Jiggins⁷⁹, J. Jimenez Pena¹⁶⁶, S. Jin^{35a}, A. Jinaru^{28b}, O. Jinnouchi¹⁵⁷, H. Jivan^{145c}, P. Johansson¹³⁹, K.A. Johns⁷, W.J. Johnson¹³⁸, K. Jon-And^{146a,146b}, G. Jones¹⁶⁹, R.W.L. Jones⁷³, S. Jones⁷, T.J. Jones⁷⁵, J. Jongmanns^{59a}, P.M. Jorge^{126a,126b}, J. Jovicevic^{159a}, X. Ju¹⁷², A. Juste Rozas^{13,r}, M.K. Köhler¹⁷¹, A. Kaczmarska⁴¹, M. Kado¹¹⁷, H. Kagan¹¹¹, M. Kagan¹⁴³, S.J. Kahn⁸⁶, T. Kaji¹⁷⁰, E. Kajomovitz⁴⁷, C.W. Kalderon¹²⁰, A. Kaluza⁸⁴, S. Kama⁴², A. Kamenshchikov¹³⁰, N. Kanaya¹⁵⁵, S. Kaneti³⁰, L. Kanjir⁷⁶, V.A. Kantserov⁹⁸, J. Kanzaki⁶⁷, B. Kaplan¹¹⁰, L.S. Kaplan¹⁷², A. Kapliy³³, D. Kar^{145c}, K. Karakostas¹⁰, A. Karamaoun³, N. Karastathis¹⁰, M.J. Kareem⁵⁶, E. Karentzos¹⁰, M. Karnevskiy⁸⁴, S.N. Karpov⁶⁶, Z.M. Karpova⁶⁶, K. Karthik¹¹⁰, V. Kartvelishvili⁷³, A.N. Karyukhin¹³⁰, K. Kasahara¹⁶⁰, L. Kashif¹⁷², R.D. Kass¹¹¹, A. Kastanas¹⁵, Y. Kataoka¹⁵⁵, C. Kato¹⁵⁵, A. Katre⁵¹, J. Katzy⁴⁴, K. Kawagoe⁷¹, T. Kawamoto¹⁵⁵, G. Kawamura⁵⁶, V.F. Kazanin^{109,c}, R. Keeler¹⁶⁸, R. Kehoe⁴², J.S. Keller⁴⁴, J.J. Kempster⁷⁸, K. Kentaro¹⁰³, H. Keoshkerian¹⁵⁸, O. Kepka¹²⁷, B.P. Kerševan⁷⁶, S. Kersten¹⁷⁴, R.A. Keyes⁸⁸, M. Khader¹⁶⁵, F. Khalil-zada¹², A. Khanov¹¹⁴, A.G. Kharlamov^{109,c}, T. Kharlamova¹⁰⁹, T.J. Khoo⁵¹, V. Khovanskiy⁹⁷, E. Khramov⁶⁶, J. Khubua^{53b,x}, S. Kido⁶⁸, C.R. Kilby⁷⁸, H.Y. Kim⁸, S.H. Kim¹⁶⁰, Y.K. Kim³³, N. Kimura¹⁵⁴, O.M. Kind¹⁷, B.T. King⁷⁵, M. King¹⁶⁶, J. Kirk¹³¹, A.E. Kiryunin¹⁰¹, T. Kishimoto¹⁵⁵, D. Kisielewska^{40a}, F. Kiss⁵⁰, K. Kiuchi¹⁶⁰, O. Kivernyk¹³⁶, E. Kladiva^{144b}, M.H. Klein³⁷, M. Klein⁷⁵, U. Klein⁷⁵, K. Kleinknecht⁸⁴, P. Klimek¹⁰⁸, A. Klimentov²⁷, R. Klingenberg⁴⁵, J.A. Klinger¹³⁹, T. Klioutchnikova³², E.-E. Kluge^{59a}, P. Kluit¹⁰⁷, S. Kluth¹⁰¹, J. Knapik⁴¹, E. Kneringer⁶³, E.B.F.G. Knoops⁸⁶, A. Knue⁵⁵, A. Kobayashi¹⁵⁵, D. Kobayashi¹⁵⁷, T. Kobayashi¹⁵⁵, M. Kobel⁴⁶, M. Kocian¹⁴³, P. Kodys¹²⁹, N.M. Koehler¹⁰¹, T. Koffas³¹, E. Koffeman¹⁰⁷, T. Koi¹⁴³, H. Kolanoski¹⁷, M. Kolb^{59b}, I. Koletsou⁵, A.A. Komar^{96,*}, Y. Komori¹⁵⁵, T. Kondo⁶⁷, N. Kondrashova⁴⁴, K. Köneke⁵⁰, A.C. König¹⁰⁶, T. Kono^{67,y}, R. Konoplich^{110,z}, N. Konstantinidis⁷⁹, R. Kopeliansky⁶², S. Koperny^{40a}, L. Köpke⁸⁴, A.K. Kopp⁵⁰, K. Korcyl⁴¹, K. Kordas¹⁵⁴, A. Korn⁷⁹, A.A. Korol^{109,c}, I. Korolkov¹³, E.V. Korolkova¹³⁹, O. Kortner¹⁰¹, S. Kortner¹⁰¹, T. Kosek¹²⁹, V.V. Kostyukhin²³, A. Kotwal⁴⁷, A. Kourkoumeli-Charalampidi^{121a,121b}, C. Kourkoumelis⁹, V. Kouskoura²⁷, A.B. Kowalewska⁴¹, R. Kowalewski¹⁶⁸, T.Z. Kowalski^{40a}, C. Kozakai¹⁵⁵, W. Kozanecki¹³⁶, A.S. Kozhin¹³⁰, V.A. Kramarenko⁹⁹, G. Kramberger⁷⁶, D. Krasnoperov⁹⁸, M.W. Krasny⁸¹, A. Krasznahorkay³², A. Kravchenko²⁷, M. Kretz^{59c}, J. Kretzschmar⁷⁵, K. Kreutzfeldt⁵⁴, P. Krieger¹⁵⁸, K. Krizka³³, K. Kroeninger⁴⁵, H. Kroha¹⁰¹, J. Kroll¹²², J. Kroseberg²³, J. Krstic¹⁴, U. Kruchonak⁶⁶, H. Krüger²³, N. Krumnack⁶⁵, M.C. Kruse⁴⁷, M. Kruskal²⁴, T. Kubota⁸⁹, H. Kucuk⁷⁹, S. Kuday^{4b}, J.T. Kuechler¹⁷⁴, S. Kuehn⁵⁰, A. Kugel^{59c}, F. Kuger¹⁷³, A. Kuhl¹³⁷, T. Kuhl⁴⁴, V. Kukhtin⁶⁶, R. Kukla¹³⁶, Y. Kulchitsky⁹³, S. Kuleshov^{34b}, M. Kuna^{132a,132b}, T. Kunigo⁶⁹, A. Kupco¹²⁷, H. Kurashige⁶⁸, Y.A. Kurochkin⁹³, V. Kus¹²⁷, E.S. Kuwertz¹⁶⁸, M. Kuze¹⁵⁷, J. Kvita¹¹⁵, T. Kwan¹⁶⁸, D. Kyriazopoulos¹³⁹, A. La Rosa¹⁰¹, J.L. La Rosa Navarro^{26d}, L. La Rotonda^{39a,39b}, C. Lacasta¹⁶⁶, F. Lacava^{132a,132b}, J. Lacey³¹, H. Lacker¹⁷, D. Lacour⁸¹, V.R. Lacuesta¹⁶⁶, E. Ladygin⁶⁶, R. Lafaye⁵, B. Laforge⁸¹, T. Lagouri¹⁷⁵, S. Lai⁵⁶, S. Lammers⁶², W. Lampl⁷, E. Lançon¹³⁶, U. Landgraf⁵⁰, M.P.J. Landon⁷⁷, M.C. Lanfermann⁵¹, V.S. Lang^{59a}, J.C. Lange¹³, A.J. Lankford¹⁶², F. Lanni²⁷, K. Lantzsck²³, A. Lanza^{121a}, S. Laplace⁸¹, C. Lapoire³², J.F. Laporte¹³⁶, T. Lari^{92a}, F. Lasagni Manghi^{22a,22b}, M. Lassnig³², P. Laurelli⁴⁹, W. Lavrijsen¹⁶, A.T. Law¹³⁷, P. Laycock⁷⁵,

T. Lazovich⁵⁸, M. Lazzaroni^{92a,92b}, B. Le⁸⁹, O. Le Dortz⁸¹, E. Le Guirriec⁸⁶, E.P. Le Quilleuc¹³⁶, M. LeBlanc¹⁶⁸, T. LeCompte⁶, F. Ledroit-Guillon⁵⁷, C.A. Lee²⁷, S.C. Lee¹⁵¹, L. Lee¹, B. Lefebvre⁸⁸, G. Lefebvre⁸¹, M. Lefebvre¹⁶⁸, F. Legger¹⁰⁰, C. Leggett¹⁶, A. Lehan⁷⁵, G. Lehmann Miotto³², X. Lei⁷, W.A. Leight³¹, A. Leisos^{154,aa}, A.G. Leister¹⁷⁵, M.A.L. Leite^{26d}, R. Leitner¹²⁹, D. Lellouch¹⁷¹, B. Lemmer⁵⁶, K.J.C. Leney⁷⁹, T. Lenz²³, B. Lenzi³², R. Leone⁷, S. Leone^{124a,124b}, C. Leonidopoulos⁴⁸, S. Leontsinis¹⁰, G. Lerner¹⁴⁹, C. Leroy⁹⁵, A.A.J. Lesage¹³⁶, C.G. Lester³⁰, M. Levchenko¹²³, J. Levêque⁵, D. Levin⁹⁰, L.J. Levinson¹⁷¹, M. Levy¹⁹, D. Lewis⁷⁷, A.M. Leyko²³, M. Leyton⁴³, B. Li^{35b,o}, C. Li^{35b}, H. Li¹⁴⁸, H.L. Li³³, L. Li⁴⁷, L. Li^{35e}, Q. Li^{35a}, S. Li⁴⁷, X. Li⁸⁵, Y. Li¹⁴¹, Z. Liang^{35a}, B. Liberti^{133a}, A. Liblong¹⁵⁸, P. Lichard³², K. Lie¹⁶⁵, J. Liebal²³, W. Liebig¹⁵, A. Limosani¹⁵⁰, S.C. Lin^{151,ab}, T.H. Lin⁸⁴, B.E. Lindquist¹⁴⁸, A.E. Lioni⁵¹, E. Lipeles¹²², A. Lipniacka¹⁵, M. Lisovyi^{59b}, T.M. Liss¹⁶⁵, A. Lister¹⁶⁷, A.M. Litke¹³⁷, B. Liu^{151,ac}, D. Liu¹⁵¹, H. Liu⁹⁰, H. Liu²⁷, J. Liu⁸⁶, J.B. Liu^{35b}, K. Liu⁸⁶, L. Liu¹⁶⁵, M. Liu⁴⁷, M. Liu^{35b}, Y.L. Liu^{35b}, Y. Liu^{35b}, M. Livan^{121a,121b}, A. Lleres⁵⁷, J. Llorente Merino^{35a}, S.L. Lloyd⁷⁷, F. Lo Sterzo¹⁵¹, E.M. Lobodzinska⁴⁴, P. Loch⁷, W.S. Lockman¹³⁷, F.K. Loebinger⁸⁵, A.E. Loeschall-Jensen³⁸, K.M. Loew²⁵, A. Loginov^{175,*}, T. Lohse¹⁷, K. Lohwasser⁴⁴, M. Lokajicek¹²⁷, B.A. Long²⁴, J.D. Long¹⁶⁵, R.E. Long⁷³, L. Longo^{74a,74b}, K.A. Looper¹¹¹, J.A. López^{34b}, D. Lopez Mateos⁵⁸, B. Lopez Paredes¹³⁹, I. Lopez Paz¹³, A. Lopez Solis⁸¹, J. Lorenz¹⁰⁰, N. Lorenzo Martinez⁶², M. Losada²¹, P.J. Lösel¹⁰⁰, X. Lou^{35a}, A. Lounis¹¹⁷, J. Love⁶, P.A. Love⁷³, H. Lu^{61a}, N. Lu⁹⁰, H.J. Lubatti¹³⁸, C. Luci^{132a,132b}, A. Lucotte⁵⁷, C. Luedtke⁵⁰, F. Luehring⁶², W. Lukas⁶³, L. Luminari^{132a}, O. Lundberg^{146a,146b}, B. Lund-Jensen¹⁴⁷, P.M. Luzi⁸¹, D. Lynn²⁷, R. Lysak¹²⁷, E. Lytken⁸², V. Lyubushkin⁶⁶, H. Ma²⁷, L.L. Ma^{35d}, Y. Ma^{35d}, G. Maccarrone⁴⁹, A. Macchiolo¹⁰¹, C.M. Macdonald¹³⁹, B. Maček⁷⁶, J. Machado Miguens^{122,126b}, D. Madaffari⁸⁶, R. Madar³⁶, H.J. Maddocks¹⁶⁴, W.F. Mader⁴⁶, A. Madsen⁴⁴, J. Maeda⁶⁸, S. Maeland¹⁵, T. Maeno²⁷, A. Maevskiy⁹⁹, E. Magradze⁵⁶, J. Mahlstedt¹⁰⁷, C. Maiani¹¹⁷, C. Maidantchik^{26a}, A.A. Maier¹⁰¹, T. Maier¹⁰⁰, A. Maio^{126a,126b,126d}, S. Majewski¹¹⁶, Y. Makida⁶⁷, N. Makovec¹¹⁷, B. Malaescu⁸¹, Pa. Malecki⁴¹, V.P. Maleev¹²³, F. Malek⁵⁷, U. Mallik⁶⁴, D. Malon⁶, C. Malone¹⁴³, C. Malone³⁰, S. Maltezos¹⁰, S. Malyukov³², J. Mamuzic¹⁶⁶, G. Mancini⁴⁹, L. Mandelli^{92a}, I. Mandić⁷⁶, J. Maneira^{126a,126b}, L. Manhaes de Andrade Filho^{26b}, J. Manjarres Ramos^{159b}, A. Mann¹⁰⁰, A. Manousos³², B. Mansoulie¹³⁶, J.D. Mansour^{35a}, R. Mantifel⁸⁸, M. Mantoani⁵⁶, S. Manzoni^{92a,92b}, L. Mapelli³², G. Marceca²⁹, L. March⁵¹, G. Marchiori⁸¹, M. Marcisovsky¹²⁷, M. Marjanovic¹⁴, D.E. Marley⁹⁰, F. Marroquin^{26a}, S.P. Marsden⁸⁵, Z. Marshall¹⁶, S. Marti-Garcia¹⁶⁶, B. Martin⁹¹, T.A. Martin¹⁶⁹, V.J. Martin⁴⁸, B. Martin dit Latour¹⁵, M. Martinez^{13,r}, V.I. Martinez Outschoorn¹⁶⁵, S. Martin-Haugh¹³¹, V.S. Martoiu^{28b}, A.C. Martyniuk⁷⁹, M. Marx¹³⁸, A. Marzin³², L. Masetti⁸⁴, T. Mashimo¹⁵⁵, R. Mashinistov⁹⁶, J. Masik⁸⁵, A.L. Maslennikov^{109,c}, I. Massa^{22a,22b}, L. Massa^{22a,22b}, P. Mastrandrea⁵, A. Mastroberardino^{39a,39b}, T. Masubuchi¹⁵⁵, P. Mättig¹⁷⁴, J. Mattmann⁸⁴, J. Maurer^{28b}, S.J. Maxfield⁷⁵, D.A. Maximov^{109,c}, R. Mazini¹⁵¹, S.M. Mazza^{92a,92b}, N.C. Mc Fadden¹⁰⁵, G. Mc Goldrick¹⁵⁸, S.P. Mc Kee⁹⁰, A. McCarn⁹⁰, R.L. McCarthy¹⁴⁸, T.G. McCarthy¹⁰¹, L.I. McClymont⁷⁹, E.F. McDonald⁸⁹, J.A. MCFayden⁷⁹, G. Mchedlize⁵⁶, S.J. McMahon¹³¹, R.A. McPherson^{168,l}, M. Medinnis⁴⁴, S. Meehan¹³⁸, S. Mehlhase¹⁰⁰, A. Mehta⁷⁵, K. Meier^{59a}, C. Meineck¹⁰⁰, B. Meirose⁴³, D. Melini¹⁶⁶, B.R. Mellado Garcia^{145c}, M. Melo^{144a}, F. Meloni¹⁸, A. Mengarelli^{22a,22b}, S. Menke¹⁰¹, E. Meoni¹⁶¹, S. Mergelmeyer¹⁷, P. Mermoud⁵¹, L. Merola^{104a,104b}, C. Meroni^{92a}, F.S. Merritt³³, A. Messina^{132a,132b}, J. Metcalfe⁶, A.S. Mete¹⁶², C. Meyer⁸⁴, C. Meyer¹²², J-P. Meyer¹³⁶, J. Meyer¹⁰⁷, H. Meyer Zu Theenhausen^{59a}, F. Miano¹⁴⁹, R.P. Middleton¹³¹, S. Miglioranza^{52a,52b}, L. Mijović⁴⁸, G. Mikenberg¹⁷¹, M. Mikestikova¹²⁷, M. Mikuž⁷⁶, M. Milesi⁸⁹, A. Milic⁶³, D.W. Miller³³, C. Mills⁴⁸, A. Milov¹⁷¹, D.A. Milstead^{146a,146b}, A.A. Minaenko¹³⁰, Y. Minami¹⁵⁵, I.A. Minashvili⁶⁶, A.I. Mincer¹¹⁰, B. Mindur^{40a}, M. Mineev⁶⁶, Y. Minegishi¹⁵⁵, Y. Ming¹⁷², L.M. Mir¹³, K.P. Mistry¹²², T. Mitani¹⁷⁰, J. Mitrevski¹⁰⁰, V.A. Mitsou¹⁶⁶, A. Miucci¹⁸, P.S. Miyagawa¹³⁹, J.U. Mjörnmark⁸², M. Mlynarikova¹²⁹, T. Moa^{146a,146b}, K. Mochizuki⁹⁵, S. Mohapatra³⁷, S. Molander^{146a,146b}, R. Moles-Valls²³, R. Monden⁶⁹, M.C. Mondragon⁹¹, K. Mönig⁴⁴, J. Monk³⁸, E. Monnier⁸⁶, A. Montalbano¹⁴⁸, J. Montejo Berlingen³², F. Monticelli⁷², S. Monzani^{92a,92b}, R.W. Moore³, N. Morange¹¹⁷, D. Moreno²¹, M. Moreno Llacer⁵⁶, P. Morettini^{52a}, S. Morgenstern³², D. Mori¹⁴², T. Mori¹⁵⁵, M. Morii⁵⁸, M. Morinaga¹⁵⁵, V. Morisbak¹¹⁹, S. Moritz⁸⁴, A.K. Morley¹⁵⁰, G. Mornacchi³², J.D. Morris⁷⁷, S.S. Mortensen³⁸, L. Morvaj¹⁴⁸, M. Mosidze^{53b}, J. Moss¹⁴³, K. Motohashi¹⁵⁷, R. Mount¹⁴³, E. Mountricha²⁷, E.J.W. Moyse⁸⁷, S. Muanza⁸⁶, R.D. Mudd¹⁹,

F. Mueller¹⁰¹, J. Mueller¹²⁵, R.S.P. Mueller¹⁰⁰, T. Mueller³⁰, D. Muenstermann⁷³, P. Mullen⁵⁵, G.A. Mullier¹⁸, F.J. Munoz Sanchez⁸⁵, J.A. Murillo Quijada¹⁹, W.J. Murray^{169,131}, H. Musheghyan⁵⁶, M. Muškinja⁷⁶, A.G. Myagkov^{130,ad}, M. Myska¹²⁸, B.P. Nachman¹⁴³, O. Nackenhorst⁵¹, K. Nagai¹²⁰, R. Nagai^{67,y}, K. Nagano⁶⁷, Y. Nagasaka⁶⁰, K. Nagata¹⁶⁰, M. Nagel⁵⁰, E. Nagy⁸⁶, A.M. Nairz³², Y. Nakahama¹⁰³, K. Nakamura⁶⁷, T. Nakamura¹⁵⁵, I. Nakano¹¹², H. Namasivayam⁴³, R.F. Naranjo Garcia⁴⁴, R. Narayan¹¹, D.I. Narrias Villar^{59a}, I. Naryshkin¹²³, T. Naumann⁴⁴, G. Navarro²¹, R. Nayyar⁷, H.A. Neal⁹⁰, P.Yu. Nechaeva⁹⁶, T.J. Neep⁸⁵, A. Negri^{121a,121b}, M. Negrini^{22a}, S. Nektarijevic¹⁰⁶, C. Nellist¹¹⁷, A. Nelson¹⁶², S. Nemecek¹²⁷, P. Nemethy¹¹⁰, A.A. Nepomuceno^{26a}, M. Nessi^{32,ae}, M.S. Neubauer¹⁶⁵, M. Neumann¹⁷⁴, R.M. Neves¹¹⁰, P. Nevski²⁷, P.R. Newman¹⁹, D.H. Nguyen⁶, T. Nguyen Manh⁹⁵, R.B. Nickerson¹²⁰, R. Nicolaidou¹³⁶, J. Nielsen¹³⁷, A. Nikiforov¹⁷, V. Nikolaenko^{130,ad}, I. Nikolic-Audit⁸¹, K. Nikolopoulos¹⁹, J.K. Nilsen¹¹⁹, P. Nilsson²⁷, Y. Ninomiya¹⁵⁵, A. Nisati^{132a}, R. Nisius¹⁰¹, T. Nobe¹⁵⁵, M. Nomachi¹¹⁸, I. Nomidis³¹, T. Nooney⁷⁷, S. Norberg¹¹³, M. Nordberg³², N. Norjoharuddeen¹²⁰, O. Novgorodova⁴⁶, S. Nowak¹⁰¹, M. Nozaki⁶⁷, L. Nozka¹¹⁵, K. Ntekas¹⁶², E. Nurse⁷⁹, F. Nuti⁸⁹, F. O'grady⁷, D.C. O'Neil¹⁴², A.A. O'Rourke⁴⁴, V. O'Shea⁵⁵, F.G. Oakham^{31,d}, H. Oberlack¹⁰¹, T. Obermann²³, J. Ocariz⁸¹, A. Ochi⁶⁸, I. Ochoa³⁷, J.P. Ochoa-Ricoux^{34a}, S. Oda⁷¹, S. Odaka⁶⁷, H. Ogren⁶², A. Oh⁸⁵, S.H. Oh⁴⁷, C.C. Ohm¹⁶, H. Ohman¹⁶⁴, H. Oide³², H. Okawa¹⁶⁰, Y. Okumura¹⁵⁵, T. Okuyama⁶⁷, A. Olariu^{28b}, L.F. Oleiro Seabra^{126a}, S.A. Olivares Pino⁴⁸, D. Oliveira Damazio²⁷, A. Olszewski⁴¹, J. Olszowska⁴¹, A. Onofre^{126a,126e}, K. Onogi¹⁰³, P.U.E. Onyisi^{11,v}, M.J. Oreglia³³, Y. Oren¹⁵³, D. Orestano^{134a,134b}, N. Orlando^{61b}, R.S. Orr¹⁵⁸, B. Osculati^{52a,52b}, R. Ospanov⁸⁵, G. Otero y Garzon²⁹, H. Otono⁷¹, M. Ouchrif^{135d}, F. Ould-Saada¹¹⁹, A. Ouraou¹³⁶, K.P. Oussoren¹⁰⁷, Q. Ouyang^{35a}, M. Owen⁵⁵, R.E. Owen¹⁹, V.E. Ozcan^{20a}, N. Ozturk⁸, K. Pachal¹⁴², A. Pacheco Pages¹³, L. Pacheco Rodriguez¹³⁶, C. Padilla Aranda¹³, M. Pagáčová⁵⁰, S. Pagan Griso¹⁶, M. Paganini¹⁷⁵, F. Paige²⁷, P. Pais⁸⁷, K. Pajchel¹¹⁹, G. Palacino^{159b}, S. Palazzo^{39a,39b}, S. Palestini³², M. Palka^{40b}, D. Pallin³⁶, E. St. Panagiotopoulou¹⁰, C.E. Pandini⁸¹, J.G. Panduro Vazquez⁷⁸, P. Pani^{146a,146b}, S. Panitkin²⁷, D. Pantea^{28b}, L. Paolozzi⁵¹, Th.D. Papadopoulou¹⁰, K. Papageorgiou¹⁵⁴, A. Paramonov⁶, D. Paredes Hernandez¹⁷⁵, A.J. Parker⁷³, M.A. Parker³⁰, K.A. Parker¹³⁹, F. Parodi^{52a,52b}, J.A. Parsons³⁷, U. Parzefall⁵⁰, V.R. Pascuzzi¹⁵⁸, E. Pasqualucci^{132a}, S. Passaggio^{52a}, Fr. Pastore⁷⁸, G. Pásztor^{31,af}, S. Pataraja¹⁷⁴, J.R. Pater⁸⁵, T. Pauly³², J. Pearce¹⁶⁸, B. Pearson¹¹³, L.E. Pedersen³⁸, M. Pedersen¹¹⁹, S. Pedraza Lopez¹⁶⁶, R. Pedro^{126a,126b}, S.V. Peleganchuk^{109,c}, O. Penc¹²⁷, C. Peng^{35a}, H. Peng^{35b}, J. Penwell⁶², B.S. Peralva^{26b}, M.M. Perego¹³⁶, D.V. Perepelitsa²⁷, E. Perez Codina^{159a}, L. Perini^{92a,92b}, H. Pernegger³², S. Perrella^{104a,104b}, R. Peschke⁴⁴, V.D. Peshekhonov⁶⁶, K. Peters⁴⁴, R.F.Y. Peters⁸⁵, B.A. Petersen³², T.C. Petersen³⁸, E. Petit⁵⁷, A. Petridis¹, C. Petridou¹⁵⁴, P. Petroff¹¹⁷, E. Petrolo^{132a}, M. Petrov¹²⁰, F. Petrucci^{134a,134b}, N.E. Pettersson⁸⁷, A. Peyaud¹³⁶, R. Pezoa^{34b}, P.W. Phillips¹³¹, G. Piacquadio^{143,ag}, E. Pianori¹⁶⁹, A. Picazio⁸⁷, E. Piccaro⁷⁷, M. Piccinini^{22a,22b}, M.A. Pickering¹²⁰, R. Piegaia²⁹, J.E. Pilcher³³, A.D. Pilkington⁸⁵, A.W.J. Pin⁸⁵, M. Pinamonti^{163a,163c,ah}, J.L. Pinfold³, A. Pingel³⁸, S. Pires⁸¹, H. Pirumov⁴⁴, M. Pitt¹⁷¹, L. Plazak^{144a}, M.-A. Pleier²⁷, V. Pleskot⁸⁴, E. Plotnikova⁶⁶, P. Plucinski⁹¹, D. Pluth⁶⁵, R. Poettgen^{146a,146b}, L. Poggioli¹¹⁷, D. Pohl²³, G. Polesello^{121a}, A. Poley⁴⁴, A. Policicchio^{39a,39b}, R. Polifka¹⁵⁸, A. Polini^{22a}, C.S. Pollard⁵⁵, V. Polychronakos²⁷, K. Pommès³², L. Pontecorvo^{132a}, B.G. Pope⁹¹, G.A. Popeneciu^{28c}, A. Poppleton³², S. Pospisil¹²⁸, K. Potamianos¹⁶, I.N. Potrap⁶⁶, C.J. Potter³⁰, C.T. Potter¹¹⁶, G. Poulard³², J. Poveda³², V. Pozdnyakov⁶⁶, M.E. Pozo Astigarraga³², P. Pralavorio⁸⁶, A. Pranko¹⁶, S. Prell⁶⁵, D. Price⁸⁵, L.E. Price⁶, M. Primavera^{74a}, S. Prince⁸⁸, K. Prokofiev^{61c}, F. Prokoshin^{34b}, S. Protopopescu²⁷, J. Proudfoot⁶, M. Przybycien^{40a}, D. Puudu^{134a,134b}, M. Purohit^{27,ai}, P. Puzo¹¹⁷, J. Qian⁹⁰, G. Qin⁵⁵, Y. Qin⁸⁵, A. Quadt⁵⁶, W.B. Quayle^{163a,163b}, M. Queitsch-Maitland⁸⁵, D. Quilty⁵⁵, S. Raddum¹¹⁹, V. Radeka²⁷, V. Radescu¹²⁰, S.K. Radhakrishnan¹⁴⁸, P. Radloff¹¹⁶, P. Rados⁸⁹, F. Ragusa^{92a,92b}, G. Rahal¹⁷⁷, J.A. Raine⁸⁵, S. Rajagopalan²⁷, M. Rammensee³², C. Rangel-Smith¹⁶⁴, M.G. Ratti^{92a,92b}, F. Rauscher¹⁰⁰, S. Rave⁸⁴, T. Ravenscroft⁵⁵, I. Ravinovich¹⁷¹, M. Raymond³², A.L. Read¹¹⁹, N.P. Readioff⁷⁵, M. Reale^{74a,74b}, D.M. Rebuzzi^{121a,121b}, A. Redelbach¹⁷³, G. Redlinger²⁷, R. Reece¹³⁷, R.G. Reed^{145c}, K. Reeves⁴³, L. Rehnisch¹⁷, J. Reichert¹²², A. Reiss⁸⁴, C. Rembser³², H. Ren^{35a}, M. Rescigno^{132a}, S. Resconi^{92a}, O.L. Rezanova^{109,c}, P. Reznicek¹²⁹, R. Rezvani⁹⁵, R. Richter¹⁰¹, S. Richter⁷⁹, E. Richter-Was^{40b}, O. Ricken²³, M. Ridel⁸¹, P. Rieck¹⁷, C.J. Riegel¹⁷⁴, J. Rieger⁵⁶, O. Rifki¹¹³, M. Rijssenbeek¹⁴⁸, A. Rimoldi^{121a,121b}, M. Rimoldi¹⁸, L. Rinaldi^{22a}, B. Ristić⁵¹, E. Ritsch³², I. Riu¹³,

F. Rizatdinova¹¹⁴, E. Rizvi⁷⁷, C. Rizzi¹³, S.H. Robertson^{88,l}, A. Robichaud-Veronneau⁸⁸, D. Robinson³⁰, J.E.M. Robinson⁴⁴, A. Robson⁵⁵, C. Roda^{124a,124b}, Y. Rodina⁸⁶, A. Rodriguez Perez¹³, D. Rodriguez Rodriguez¹⁶⁶, S. Roe³², C.S. Rogan⁵⁸, O. Røhne¹¹⁹, A. Romaniouk⁹⁸, M. Romano^{22a,22b}, S.M. Romano Saez³⁶, E. Romero Adam¹⁶⁶, N. Rompotis¹³⁸, M. Ronzani⁵⁰, L. Roos⁸¹, E. Ros¹⁶⁶, S. Rosati^{132a}, K. Rosbach⁵⁰, P. Rose¹³⁷, N.-A. Rosien⁵⁶, V. Rossetti^{146a,146b}, E. Rossi^{104a,104b}, L.P. Rossi^{52a}, J.H.N. Rosten³⁰, R. Rosten¹³⁸, M. Rotaru^{28b}, I. Roth¹⁷¹, J. Rothberg¹³⁸, D. Rousseau¹¹⁷, A. Rozanov⁸⁶, Y. Rozen¹⁵², X. Ruan^{145c}, F. Rubbo¹⁴³, M.S. Rudolph¹⁵⁸, F. Rühr⁵⁰, A. Ruiz-Martinez³¹, Z. Rurikova⁵⁰, N.A. Rusakovich⁶⁶, A. Ruschke¹⁰⁰, H.L. Russell¹³⁸, J.P. Rutherford⁷, N. Ruthmann³², Y.F. Ryabov¹²³, M. Rybar¹⁶⁵, G. Rybkin¹¹⁷, S. Ryu⁶, A. Ryzhov¹³⁰, G.F. Rzehorz⁵⁶, A.F. Saavedra¹⁵⁰, G. Sabato¹⁰⁷, S. Sacerdoti²⁹, H.F.-W. Sadrozinski¹³⁷, R. Sadykov⁶⁶, F. Safai Tehrani^{132a}, P. Saha¹⁰⁸, M. Sahinsoy^{59a}, M. Saimpert¹³⁶, T. Saito¹⁵⁵, H. Sakamoto¹⁵⁵, Y. Sakurai¹⁷⁰, G. Salamanna^{134a,134b}, A. Salamon^{133a,133b}, J.E. Salazar Loyola^{34b}, D. Salek¹⁰⁷, P.H. Sales De Bruin¹³⁸, D. Salihagic¹⁰¹, A. Salsnikov¹⁴³, J. Salt¹⁶⁶, D. Salvatore^{39a,39b}, F. Salvatore¹⁴⁹, A. Salvucci^{61a}, A. Salzburger³², D. Sammel⁵⁰, D. Sampsonidis¹⁵⁴, A. Sanchez^{104a,104b}, J. Sánchez¹⁶⁶, V. Sanchez Martinez¹⁶⁶, H. Sandaker¹¹⁹, R.L. Sandbach⁷⁷, H.G. Sander⁸⁴, M. Sandhoff¹⁷⁴, C. Sandoval²¹, D.P.C. Sankey¹³¹, M. Sannino^{52a,52b}, A. Sansoni⁴⁹, C. Santoni³⁶, R. Santonico^{133a,133b}, H. Santos^{126a}, I. Santoyo Castillo¹⁴⁹, K. Sapp¹²⁵, A. Saproonov⁶⁶, J.G. Saraiva^{126a,126d}, B. Sarrazin²³, O. Sasaki⁶⁷, K. Sato¹⁶⁰, E. Sauvan⁵, G. Savage⁷⁸, P. Savard^{158,d}, N. Savic¹⁰¹, C. Sawyer¹³¹, L. Sawyer^{80,q}, J. Saxon³³, C. Sbarra^{22a}, A. Sbrizzi^{22a,22b}, T. Scanlon⁷⁹, D.A. Scannicchio¹⁶², M. Scarcella¹⁵⁰, V. Scarfone^{39a,39b}, J. Schaarschmidt¹⁷¹, P. Schacht¹⁰¹, B.M. Schachtner¹⁰⁰, D. Schaefer³², L. Schaefer¹²², R. Schaefer⁴⁴, J. Schaeffer⁸⁴, S. Schaepe²³, S. Schaezel^{59b}, U. Schäfer⁸⁴, A.C. Schaffer¹¹⁷, D. Schaile¹⁰⁰, R.D. Schamberger¹⁴⁸, V. Scharf^{59a}, V.A. Schegelsky¹²³, D. Scheirich¹²⁹, M. Schernau¹⁶², C. Schiavi^{52a,52b}, S. Schier¹³⁷, C. Schillo⁵⁰, M. Schioppa^{39a,39b}, S. Schlenker³², K.R. Schmidt-Sommerfeld¹⁰¹, K. Schmieden³², C. Schmitt⁸⁴, S. Schmitt⁴⁴, S. Schmitz⁸⁴, B. Schneider^{159a}, U. Schnoor⁵⁰, L. Schoeffel¹³⁶, A. Schoening^{59b}, B.D. Schoenrock⁹¹, E. Schopf²³, M. Schott⁸⁴, J. Schovancova⁸, S. Schramm⁵¹, M. Schreyer¹⁷³, N. Schuh⁸⁴, A. Schulte⁸⁴, M.J. Schultens²³, H.-C. Schultz-Coulon^{59a}, H. Schulz¹⁷, M. Schumacher⁵⁰, B.A. Schumm¹³⁷, Ph. Schune¹³⁶, A. Schwartzman¹⁴³, T.A. Schwarz⁹⁰, H. Schweiger⁸⁵, Ph. Schwemling¹³⁶, R. Schwienhorst⁹¹, J. Schwindling¹³⁶, T. Schwindt²³, G. Sciolla²⁵, F. Scuri^{124a,124b}, F. Scutti⁸⁹, J. Searcy⁹⁰, P. Seema²³, S.C. Seidel¹⁰⁵, A. Seiden¹³⁷, F. Seifert¹²⁸, J.M. Seixas^{26a}, G. Sekhniaidze^{104a}, K. Sekhon⁹⁰, S.J. Sekula⁴², D.M. Seliverstov^{123,*}, N. Semprini-Cesari^{22a,22b}, C. Serfon¹¹⁹, L. Serin¹¹⁷, L. Serkin^{163a,163b}, M. Sessa^{134a,134b}, R. Seuster¹⁶⁸, H. Severini¹¹³, T. Sfiligoj⁷⁶, F. Sforza³², A. Sfyrla⁵¹, E. Shabalina⁵⁶, N.W. Shaikh^{146a,146b}, L.Y. Shan^{35a}, R. Shang¹⁶⁵, J.T. Shank²⁴, M. Shapiro¹⁶, P.B. Shatalov⁹⁷, K. Shaw^{163a,163b}, S.M. Shaw⁸⁵, A. Shcherbakova^{146a,146b}, C.Y. Shehu¹⁴⁹, P. Sherwood⁷⁹, L. Shi^{151,aj}, S. Shimizu⁶⁸, C.O. Shimmin¹⁶², M. Shimojima¹⁰², S. Shirabe⁷¹, M. Shiyakova^{66,ak}, A. Shmeleva⁹⁶, D. Shoaleh Saadi⁹⁵, M.J. Shochet³³, S. Shojaii^{92a,92b}, D.R. Shope¹¹³, S. Shrestha¹¹¹, E. Shulga⁹⁸, M.A. Shupe⁷, P. Sicho¹²⁷, A.M. Sickles¹⁶⁵, P.E. Sidebo¹⁴⁷, O. Sidiropoulou¹⁷³, D. Sidorov¹¹⁴, A. Sidoti^{22a,22b}, F. Siegert⁴⁶, Dj. Sijacki¹⁴, J. Silva^{126a,126d}, S.B. Silverstein^{146a}, V. Simak¹²⁸, Lj. Simic¹⁴, S. Simion¹¹⁷, E. Simioni⁸⁴, B. Simmons⁷⁹, D. Simon³⁶, M. Simon⁸⁴, P. Sinervo¹⁵⁸, N.B. Sinev¹¹⁶, M. Sioli^{22a,22b}, G. Siragusa¹⁷³, S.Yu. Sivoklov⁹⁹, J. Sjölin^{146a,146b}, M.B. Skinner⁷³, H.P. Skottowe⁵⁸, P. Skubic¹¹³, M. Slater¹⁹, T. Slavicek¹²⁸, M. Slawinska¹⁰⁷, K. Sliwa¹⁶¹, R. Slovak¹²⁹, V. Smakhtin¹⁷¹, B.H. Smart⁵, L. Smestad¹⁵, J. Smiesko^{144a}, S.Yu. Smirnov⁹⁸, Y. Smirnov⁹⁸, L.N. Smirnova^{99,al}, O. Smirnova⁸², M.N.K. Smith³⁷, R.W. Smith³⁷, M. Smizanska⁷³, K. Smolek¹²⁸, A.A. Snesev⁹⁶, I.M. Snyder¹¹⁶, S. Snyder²⁷, R. Sobie^{168,l}, F. Socher⁴⁶, A. Soffer¹⁵³, D.A. Soh¹⁵¹, G. Sokhrannyi⁷⁶, C.A. Solans Sanchez³², M. Solar¹²⁸, E.Yu. Soldatov⁹⁸, U. Soldevila¹⁶⁶, A.A. Solodkov¹³⁰, A. Soloshenko⁶⁶, O.V. Solovyanov¹³⁰, V. Solovyev¹²³, P. Sommer⁵⁰, H. Son¹⁶¹, H.Y. Song^{35b,am}, A. Sood¹⁶, A. Sopczak¹²⁸, V. Sopko¹²⁸, V. Sorin¹³, D. Sosa^{59b}, C.L. Sotiropoulou^{124a,124b}, R. Soualah^{163a,163c}, A.M. Soukharev^{109,c}, D. South⁴⁴, B.C. Sowden⁷⁸, S. Spagnolo^{74a,74b}, M. Spalla^{124a,124b}, M. Spangenberg¹⁶⁹, F. Spanò⁷⁸, D. Sperlich¹⁷, F. Spettel¹⁰¹, R. Spighi^{22a}, G. Spigo³², L.A. Spiller⁸⁹, M. Spousta¹²⁹, R.D. St. Denis^{55,*}, A. Stabile^{92a}, R. Stamen^{59a}, S. Stamm¹⁷, E. Stanecka⁴¹, R.W. Stanek⁶, C. Stanescu^{134a}, M. Stanescu-Bellu⁴⁴, M.M. Stanitzki⁴⁴, S. Stapnes¹¹⁹, E.A. Starchenko¹³⁰, G.H. Stark³³, J. Stark⁵⁷, P. Staroba¹²⁷, P. Starovoitov^{59a}, S. Stärz³², R. Staszewski⁴¹, P. Steinberg²⁷, B. Stelzer¹⁴², H.J. Stelzer³², O. Stelzer-Chilton^{159a}, H. Stenzel⁵⁴, G.A. Stewart⁵⁵, J.A. Stillings²³,

M.C. Stockton⁸⁸, M. Stoebe⁸⁸, G. Stoicea^{28b}, P. Stolte⁵⁶, S. Stonjek¹⁰¹, A.R. Stradling⁸, A. Straessner⁴⁶,
 M.E. Stramaglia¹⁸, J. Strandberg¹⁴⁷, S. Strandberg^{146a,146b}, A. Strandlie¹¹⁹, M. Strauss¹¹³,
 P. Strizenec^{144b}, R. Ströhmer¹⁷³, D.M. Strom¹¹⁶, R. Stroynowski⁴², A. Strubig¹⁰⁶, S.A. Stucci²⁷,
 B. Stugu¹⁵, N.A. Styles⁴⁴, D. Su¹⁴³, J. Su¹²⁵, S. Suchek^{59a}, Y. Sugaya¹¹⁸, M. Suk¹²⁸, V.V. Sulin⁹⁶,
 S. Sultansoy^{4c}, T. Sumida⁶⁹, S. Sun⁵⁸, X. Sun^{35a}, J.E. Sundermann⁵⁰, K. Suruliz¹⁴⁹, G. Susinno^{39a,39b},
 M.R. Sutton¹⁴⁹, S. Suzuki⁶⁷, M. Svatos¹²⁷, M. Swiatlowski³³, I. Sykora^{144a}, T. Sykora¹²⁹, D. Ta⁵⁰,
 C. Taccini^{134a,134b}, K. Tackmann⁴⁴, J. Taenzer¹⁵⁸, A. Taffard¹⁶², R. Tafirout^{159a}, N. Taiblum¹⁵³,
 H. Takai²⁷, R. Takashima⁷⁰, T. Takeshita¹⁴⁰, Y. Takubo⁶⁷, M. Talby⁸⁶, A.A. Talyshv^{109,c}, K.G. Tan⁸⁹,
 J. Tanaka¹⁵⁵, M. Tanaka¹⁵⁷, R. Tanaka¹¹⁷, S. Tanaka⁶⁷, R. Tanioka⁶⁸, B.B. Tannenwald¹¹¹,
 S. Tapia Araya^{34b}, S. Tapprogge⁸⁴, S. Tarem¹⁵², G.F. Tartarelli^{92a}, P. Tas¹²⁹, M. Tasevsky¹²⁷, T. Tashiro⁶⁹,
 E. Tassi^{39a,39b}, A. Tavares Delgado^{126a,126b}, Y. Tayalati^{135e}, A.C. Taylor¹⁰⁵, G.N. Taylor⁸⁹, P.T.E. Taylor⁸⁹,
 W. Taylor^{159b}, F.A. Teischinger³², P. Teixeira-Dias⁷⁸, K.K. Temming⁵⁰, D. Temple¹⁴², H. Ten Kate³²,
 P.K. Teng¹⁵¹, J.J. Teoh¹¹⁸, F. Tepel¹⁷⁴, S. Terada⁶⁷, K. Terashi¹⁵⁵, J. Terron⁸³, S. Terzo¹³, M. Testa⁴⁹,
 R.J. Teuscher^{158,l}, T. Theveneaux-Pelzer⁸⁶, J.P. Thomas¹⁹, J. Thomas-Wilsker⁷⁸, E.N. Thompson³⁷,
 P.D. Thompson¹⁹, A.S. Thompson⁵⁵, L.A. Thomsen¹⁷⁵, E. Thomson¹²², M. Thomson³⁰, M.J. Tibbetts¹⁶,
 R.E. Tisce Torres⁸⁶, V.O. Tikhomirov^{96,an}, Yu.A. Tikhonov^{109,c}, S. Timoshenko⁹⁸, P. Tipton¹⁷⁵,
 S. Tisserant⁸⁶, K. Todome¹⁵⁷, T. Todorov^{5,*}, S. Todorova-Nova¹²⁹, J. Tojo⁷¹, S. Tokár^{144a},
 K. Tokushuku⁶⁷, E. Tolley⁵⁸, L. Tomlinson⁸⁵, M. Tomoto¹⁰³, L. Tompkins^{143,ao}, K. Toms¹⁰⁵, B. Tong⁵⁸,
 P. Tornambe⁵⁰, E. Torrence¹¹⁶, H. Torres¹⁴², E. Torrón Pastor¹³⁸, J. Toth^{86,ap}, F. Touchard⁸⁶,
 D.R. Tovey¹³⁹, T. Trefzger¹⁷³, A. Tricoli²⁷, I.M. Trigger^{159a}, S. Trincaz-Duvoid⁸¹, M.F. Tripiana¹³,
 W. Trischuk¹⁵⁸, B. Trocmé⁵⁷, A. Trofymov⁴⁴, C. Troncon^{92a}, M. Trotter-McDonald¹⁶, M. Trovatelli¹⁶⁸,
 L. Truong^{163a,163c}, M. Trzebinski⁴¹, A. Trzupek⁴¹, J.C-L. Tseng¹²⁰, P.V. Tsiareshka⁹³, G. Tsipolitis¹⁰,
 N. Tsirintanis⁹, S. Tsiskaridze¹³, V. Tsiskaridze⁵⁰, E.G. Tskhadadze^{53a}, K.M. Tsui^{61a}, I.I. Tsukerman⁹⁷,
 V. Tsulaia¹⁶, S. Tsuno⁶⁷, D. Tsybychev¹⁴⁸, Y. Tu^{61b}, A. Tudorache^{28b}, V. Tudorache^{28b}, A.N. Tuna⁵⁸,
 S.A. Tupputi^{22a,22b}, S. Turchikhin⁶⁶, D. Turecek¹²⁸, D. Turgeman¹⁷¹, R. Turra^{92a,92b}, P.M. Tuts³⁷,
 M. Tyndel¹³¹, G. Uchielli^{22a,22b}, I. Ueda¹⁵⁵, M. Ughetto^{146a,146b}, F. Ukegawa¹⁶⁰, G. Unal³²,
 A. Undrus²⁷, G. Unel¹⁶², F.C. Ungaro⁸⁹, Y. Unno⁶⁷, C. Unverdorben¹⁰⁰, J. Urban^{144b}, P. Urquijo⁸⁹,
 P. Urrejola⁸⁴, G. Usai⁸, L. Vacavant⁸⁶, V. Vacek¹²⁸, B. Vachon⁸⁸, C. Valderanis¹⁰⁰,
 E. Valdes Santurio^{146a,146b}, N. Valencic¹⁰⁷, S. Valentinetti^{22a,22b}, A. Valero¹⁶⁶, L. Valery¹³, S. Valkar¹²⁹,
 J.A. Valls Ferrer¹⁶⁶, W. Van Den Wollenberg¹⁰⁷, P.C. Van Der Deijl¹⁰⁷, H. van der Graaf¹⁰⁷,
 N. van Eldik¹⁵², P. van Gemmeren⁶, J. Van Nieuwkoop¹⁴², I. van Vulpen¹⁰⁷, M.C. van Woerden³²,
 M. Vanadia^{132a,132b}, W. Vandelli³², R. Vanguri¹²², A. Vaniachine¹³⁰, P. Vankov¹⁰⁷, G. Vardanyan¹⁷⁶,
 R. Vari^{132a}, E.W. Varnes⁷, T. Varol⁴², D. Varouchas⁸¹, A. Vartapetian⁸, K.E. Varvell¹⁵⁰, J.G. Vasquez¹⁷⁵,
 G.A. Vasquez^{34b}, F. Vazeille³⁶, T. Vazquez Schroeder⁸⁸, J. Veatch⁵⁶, V. Veeraraghavan⁷, L.M. Veloce¹⁵⁸,
 F. Veloso^{126a,126c}, S. Veneziano^{132a}, A. Ventura^{74a,74b}, M. Venturi¹⁶⁸, N. Venturi¹⁵⁸, A. Venturini²⁵,
 V. Vercesi^{121a}, M. Verducci^{132a,132b}, W. Verkerke¹⁰⁷, J.C. Vermeulen¹⁰⁷, A. Vest^{46,aq}, M.C. Vetterli^{142,d},
 O. Viazlo⁸², I. Vichou^{165,*}, T. Vickey¹³⁹, O.E. Vickey Boeriu¹³⁹, G.H.A. Viehhauser¹²⁰, S. Viel¹⁶,
 L. Vigani¹²⁰, M. Villa^{22a,22b}, M. Villaplana Perez^{92a,92b}, E. Vilucchi⁴⁹, M.G. Vincter³¹, V.B. Vinogradov⁶⁶,
 C. Vittori^{22a,22b}, I. Vivarelli¹⁴⁹, S. Vlachos¹⁰, M. Vlasak¹²⁸, M. Vogel¹⁷⁴, P. Vokac¹²⁸, G. Volpi^{124a,124b},
 M. Volpi⁸⁹, H. von der Schmitt¹⁰¹, E. von Toerne²³, V. Vorobel¹²⁹, K. Vorobev⁹⁸, M. Vos¹⁶⁶, R. Voss³²,
 J.H. Vosseveld⁷⁵, N. Vranjes¹⁴, M. Vranjes Milosavljevic¹⁴, V. Vrba¹²⁷, M. Vreeswijk¹⁰⁷, R. Vuillemet³²,
 I. Vukotic³³, Z. Vykydal¹²⁸, P. Wagner²³, W. Wagner¹⁷⁴, H. Wahlberg⁷², S. Wahrenmund⁴⁶,
 J. Wakabayashi¹⁰³, J. Walder⁷³, R. Walker¹⁰⁰, W. Walkowiak¹⁴¹, V. Wallangen^{146a,146b}, C. Wang^{35c},
 C. Wang^{35d,86}, F. Wang¹⁷², H. Wang¹⁶, H. Wang⁴², J. Wang⁴⁴, J. Wang¹⁵⁰, K. Wang⁸⁸, R. Wang⁶,
 S.M. Wang¹⁵¹, T. Wang²³, T. Wang³⁷, W. Wang^{35b}, X. Wang¹⁷⁵, C. Wanotayaroj¹¹⁶, A. Warburton⁸⁸,
 C.P. Ward³⁰, D.R. Wardrope⁷⁹, A. Washbrook⁴⁸, P.M. Watkins¹⁹, A.T. Watson¹⁹, M.F. Watson¹⁹,
 G. Watts¹³⁸, S. Watts⁸⁵, B.M. Waugh⁷⁹, S. Webb⁸⁴, M.S. Weber¹⁸, S.W. Weber¹⁷³, S.A. Weber³¹,
 J.S. Webster⁶, A.R. Weidberg¹²⁰, B. Weinert⁶², J. Weingarten⁵⁶, C. Weiser⁵⁰, H. Weits¹⁰⁷, P.S. Wells³²,
 T. Wenaus²⁷, T. Wengler³², S. Wenig³², N. Wermes²³, M. Werner⁵⁰, M.D. Werner⁶⁵, P. Werner³²,
 M. Wessels^{59a}, J. Wetter¹⁶¹, K. Whalen¹¹⁶, N.L. Whallon¹³⁸, A.M. Wharton⁷³, A. White⁸, M.J. White¹,
 R. White^{34b}, D. Whiteson¹⁶², F.J. Wickens¹³¹, W. Wiedenmann¹⁷², M. Wielers¹³¹, C. Wiglesworth³⁸,
 L.A.M. Wiik-Fuchs²³, A. Wildauer¹⁰¹, F. Wilk⁸⁵, H.G. Wilkens³², H.H. Williams¹²², S. Williams¹⁰⁷,

C. Willis⁹¹, S. Willocq⁸⁷, J.A. Wilson¹⁹, I. Wingerter-Seez⁵, F. Winklmeier¹¹⁶, O.J. Winston¹⁴⁹, B.T. Winter²³, M. Wittgen¹⁴³, J. Wittkowski¹⁰⁰, T.M.H. Wolf¹⁰⁷, M.W. Wolter⁴¹, H. Wolters^{126a,126c}, S.D. Worm¹³¹, B.K. Wosiek⁴¹, J. Wotschack³², M.J. Woudstra⁸⁵, K.W. Wozniak⁴¹, M. Wu⁵⁷, M. Wu³³, S.L. Wu¹⁷², X. Wu⁵¹, Y. Wu⁹⁰, T.R. Wyatt⁸⁵, B.M. Wynne⁴⁸, S. Xella³⁸, D. Xu^{35a}, L. Xu²⁷, B. Yabsley¹⁵⁰, S. Yacoob^{145a}, D. Yamaguchi¹⁵⁷, Y. Yamaguchi¹¹⁸, A. Yamamoto⁶⁷, S. Yamamoto¹⁵⁵, T. Yamanaka¹⁵⁵, K. Yamauchi¹⁰³, Y. Yamazaki⁶⁸, Z. Yan²⁴, H. Yang^{35e}, H. Yang¹⁷², Y. Yang¹⁵¹, Z. Yang¹⁵, W.-M. Yao¹⁶, Y.C. Yap⁸¹, Y. Yasu⁶⁷, E. Yatsenko⁵, K.H. Yau Wong²³, J. Ye⁴², S. Ye²⁷, I. Yeletsikh⁶⁶, A.L. Yen⁵⁸, E. Yildirim⁸⁴, K. Yorita¹⁷⁰, R. Yoshida⁶, K. Yoshihara¹²², C. Young¹⁴³, C.J.S. Young³², S. Youssef²⁴, D.R. Yu¹⁶, J. Yu⁸, J.M. Yu⁹⁰, J. Yu⁶⁵, L. Yuan⁶⁸, S.P.Y. Yuen²³, I. Yusuff^{30,ar}, B. Zabinski⁴¹, R. Zaidan⁶⁴, A.M. Zaitsev^{130,ad}, N. Zakharchuk⁴⁴, J. Zalieckas¹⁵, A. Zaman¹⁴⁸, S. Zambito⁵⁸, L. Zanello^{132a,132b}, D. Zanzi⁸⁹, C. Zeitnitz¹⁷⁴, M. Zeman¹²⁸, A. Zemla^{40a}, J.C. Zeng¹⁶⁵, Q. Zeng¹⁴³, K. Zengel²⁵, O. Zenin¹³⁰, T. Ženiš^{144a}, D. Zerwas¹¹⁷, D. Zhang⁹⁰, F. Zhang¹⁷², G. Zhang^{35b,am}, H. Zhang^{35c}, J. Zhang⁶, L. Zhang⁵⁰, R. Zhang²³, R. Zhang^{35b,as}, X. Zhang^{35d}, Z. Zhang¹¹⁷, X. Zhao⁴², Y. Zhao^{35d}, Z. Zhao^{35b}, A. Zhemchugov⁶⁶, J. Zhong¹²⁰, B. Zhou⁹⁰, C. Zhou¹⁷², L. Zhou³⁷, L. Zhou⁴², M. Zhou¹⁴⁸, N. Zhou^{35f}, C.G. Zhu^{35d}, H. Zhu^{35a}, J. Zhu⁹⁰, Y. Zhu^{35b}, X. Zhuang^{35a}, K. Zhukov⁹⁶, A. Zibell¹⁷³, D. Zieminska⁶², N.I. Zimine⁶⁶, C. Zimmermann⁸⁴, S. Zimmermann⁵⁰, Z. Zinonos⁵⁶, M. Zinser⁸⁴, M. Ziolkowski¹⁴¹, L. Živković¹⁴, G. Zobernig¹⁷², A. Zoccoli^{22a,22b}, M. zur Nedden¹⁷, L. Zwalinski³²

¹ Department of Physics, University of Adelaide, Adelaide, Australia

² Physics Department, SUNY Albany, Albany, NY, United States

³ Department of Physics, University of Alberta, Edmonton, AB, Canada

⁴ (a) Department of Physics, Ankara University, Ankara; (b) Istanbul Aydin University, Istanbul; (c) Division of Physics, TOBB University of Economics and Technology, Ankara, Turkey

⁵ LAPP, CNRS/IN2P3 and Université Savoie Mont Blanc, Annecy-le-Vieux, France

⁶ High Energy Physics Division, Argonne National Laboratory, Argonne, IL, United States

⁷ Department of Physics, University of Arizona, Tucson, AZ, United States

⁸ Department of Physics, The University of Texas at Arlington, Arlington, TX, United States

⁹ Physics Department, University of Athens, Athens, Greece

¹⁰ Physics Department, National Technical University of Athens, Zografou, Greece

¹¹ Department of Physics, The University of Texas at Austin, Austin, TX, United States

¹² Institute of Physics, Azerbaijan Academy of Sciences, Baku, Azerbaijan

¹³ Institut de Física d'Altes Energies (IFAE), The Barcelona Institute of Science and Technology, Barcelona, Spain

¹⁴ Institute of Physics, University of Belgrade, Belgrade, Serbia

¹⁵ Department for Physics and Technology, University of Bergen, Bergen, Norway

¹⁶ Physics Division, Lawrence Berkeley National Laboratory and University of California, Berkeley, CA, United States

¹⁷ Department of Physics, Humboldt University, Berlin, Germany

¹⁸ Albert Einstein Center for Fundamental Physics and Laboratory for High Energy Physics, University of Bern, Bern, Switzerland

¹⁹ School of Physics and Astronomy, University of Birmingham, Birmingham, United Kingdom

²⁰ (a) Department of Physics, Bogazici University, Istanbul; (b) Department of Physics Engineering, Gaziantep University, Gaziantep; (d) Istanbul Bilgi University, Faculty of Engineering and Natural Sciences, Istanbul, Turkey; (e) Bahcesehir University, Faculty of Engineering and Natural Sciences, Istanbul, Turkey

²¹ Centro de Investigaciones, Universidad Antonio Narino, Bogota, Colombia

²² (a) INFN Sezione di Bologna; (b) Dipartimento di Fisica e Astronomia, Università di Bologna, Bologna, Italy

²³ Physikalisches Institut, University of Bonn, Bonn, Germany

²⁴ Department of Physics, Boston University, Boston, MA, United States

²⁵ Department of Physics, Brandeis University, Waltham, MA, United States

²⁶ (a) Universidade Federal do Rio De Janeiro COPPE/EE/IF, Rio de Janeiro; (b) Electrical Circuits Department, Federal University of Juiz de Fora (UFJF), Juiz de Fora; (c) Federal University of Sao Joao del Rei (UFSJ), Sao Joao del Rei; (d) Instituto de Fisica, Universidade de Sao Paulo, Sao Paulo, Brazil

²⁷ Physics Department, Brookhaven National Laboratory, Upton, NY, United States

²⁸ (a) Transilvania University of Brasov, Brasov, Romania; (b) National Institute of Physics and Nuclear Engineering, Bucharest; (c) National Institute for Research and Development of Isotopic and Molecular Technologies, Physics Department, Cluj Napoca; (d) University Politehnica Bucharest, Bucharest; (e) West University in Timisoara, Timisoara, Romania

²⁹ Departamento de Física, Universidad de Buenos Aires, Buenos Aires, Argentina

³⁰ Cavendish Laboratory, University of Cambridge, Cambridge, United Kingdom

³¹ Department of Physics, Carleton University, Ottawa, ON, Canada

³² CERN, Geneva, Switzerland

³³ Enrico Fermi Institute, University of Chicago, Chicago, IL, United States

³⁴ (a) Departamento de Física, Pontificia Universidad Católica de Chile, Santiago; (b) Departamento de Física, Universidad Técnica Federico Santa María, Valparaíso, Chile

³⁵ (a) Institute of High Energy Physics, Chinese Academy of Sciences, Beijing; (b) Department of Modern Physics, University of Science and Technology of China, Anhui; (c) Department of Physics, Nanjing University, Jiangsu; (d) School of Physics, Shandong University, Shandong; (e) Department of Physics and Astronomy, Shanghai Key Laboratory for Particle Physics and Cosmology, Shanghai Jiao Tong University, Shanghai; (f) Physics Department, Tsinghua University, Beijing 100084, China

³⁶ Laboratoire de Physique Corpusculaire, Clermont Université and Université Blaise Pascal and CNRS/IN2P3, Clermont-Ferrand, France

³⁷ Nevis Laboratory, Columbia University, Irvington, NY, United States

³⁸ Niels Bohr Institute, University of Copenhagen, Copenhagen, Denmark

³⁹ (a) INFN Gruppo Collegato di Cosenza, Laboratori Nazionali di Frascati; (b) Dipartimento di Fisica, Università della Calabria, Rende, Italy

⁴⁰ (a) AGH University of Science and Technology, Faculty of Physics and Applied Computer Science, Krakow; (b) Marian Smoluchowski Institute of Physics, Jagiellonian University, Krakow, Poland

⁴¹ Institute of Nuclear Physics Polish Academy of Sciences, Krakow, Poland

⁴² Physics Department, Southern Methodist University, Dallas, TX, United States

⁴³ Physics Department, University of Texas at Dallas, Richardson, TX, United States

⁴⁴ DESY, Hamburg and Zeuthen, Germany

⁴⁵ Lehrstuhl für Experimentelle Physik IV, Technische Universität Dortmund, Dortmund, Germany

⁴⁶ Institut für Kern- und Teilchenphysik, Technische Universität Dresden, Dresden, Germany

⁴⁷ Department of Physics, Duke University, Durham, NC, United States

- 48 SUPA – School of Physics and Astronomy, University of Edinburgh, Edinburgh, United Kingdom
- 49 INFN Laboratori Nazionali di Frascati, Frascati, Italy
- 50 Fakultät für Mathematik und Physik, Albert-Ludwigs-Universität, Freiburg, Germany
- 51 Section de Physique, Université de Genève, Geneva, Switzerland
- 52 (a) INFN Sezione di Genova; (b) Dipartimento di Fisica, Università di Genova, Genova, Italy
- 53 (a) E. Andronikashvili Institute of Physics, Iv. Javakishvili Tbilisi State University, Tbilisi; (b) High Energy Physics Institute, Tbilisi State University, Tbilisi, Georgia
- 54 II Physikalisches Institut, Justus-Liebig-Universität Giessen, Giessen, Germany
- 55 SUPA – School of Physics and Astronomy, University of Glasgow, Glasgow, United Kingdom
- 56 II Physikalisches Institut, Georg-August-Universität, Göttingen, Germany
- 57 Laboratoire de Physique Subatomique et de Cosmologie, Université Grenoble-Alpes, CNRS/IN2P3, Grenoble, France
- 58 Laboratory for Particle Physics and Cosmology, Harvard University, Cambridge, MA, United States
- 59 (a) Kirchhoff-Institut für Physik, Ruprecht-Karls-Universität Heidelberg, Heidelberg; (b) Physikalisches Institut, Ruprecht-Karls-Universität Heidelberg, Heidelberg; (c) ZITI Institut für technische Informatik, Ruprecht-Karls-Universität Heidelberg, Mannheim, Germany
- 60 Faculty of Applied Information Science, Hiroshima Institute of Technology, Hiroshima, Japan
- 61 (a) Department of Physics, The Chinese University of Hong Kong, Shatin, N.T., Hong Kong; (b) Department of Physics, The University of Hong Kong, Hong Kong; (c) Department of Physics, The Hong Kong University of Science and Technology, Clear Water Bay, Kowloon, Hong Kong, China
- 62 Department of Physics, Indiana University, Bloomington, IN, United States
- 63 Institut für Astro- und Teilchenphysik, Leopold-Franzens-Universität, Innsbruck, Austria
- 64 University of Iowa, Iowa City, IA, United States
- 65 Department of Physics and Astronomy, Iowa State University, Ames, IA, United States
- 66 Joint Institute for Nuclear Research, JINR Dubna, Dubna, Russia
- 67 KEK, High Energy Accelerator Research Organization, Tsukuba, Japan
- 68 Graduate School of Science, Kobe University, Kobe, Japan
- 69 Faculty of Science, Kyoto University, Kyoto, Japan
- 70 Kyoto University of Education, Kyoto, Japan
- 71 Department of Physics, Kyushu University, Fukuoka, Japan
- 72 Instituto de Física La Plata, Universidad Nacional de La Plata and CONICET, La Plata, Argentina
- 73 Physics Department, Lancaster University, Lancaster, United Kingdom
- 74 (a) INFN Sezione di Lecce; (b) Dipartimento di Matematica e Fisica, Università del Salento, Lecce, Italy
- 75 Oliver Lodge Laboratory, University of Liverpool, Liverpool, United Kingdom
- 76 Department of Physics, Jožef Stefan Institute and University of Ljubljana, Ljubljana, Slovenia
- 77 School of Physics and Astronomy, Queen Mary University of London, London, United Kingdom
- 78 Department of Physics, Royal Holloway University of London, Surrey, United Kingdom
- 79 Department of Physics and Astronomy, University College London, London, United Kingdom
- 80 Louisiana Tech University, Ruston, LA, United States
- 81 Laboratoire de Physique Nucléaire et de Hautes Energies, UPMC and Université Paris-Diderot and CNRS/IN2P3, Paris, France
- 82 Fysiska Institutionen, Lunds Universitet, Lund, Sweden
- 83 Departamento de Física Teórica C-15, Universidad Autónoma de Madrid, Madrid, Spain
- 84 Institut für Physik, Universität Mainz, Mainz, Germany
- 85 School of Physics and Astronomy, University of Manchester, Manchester, United Kingdom
- 86 CPPM, Aix-Marseille Université and CNRS/IN2P3, Marseille, France
- 87 Department of Physics, University of Massachusetts, Amherst, MA, United States
- 88 Department of Physics, McGill University, Montreal, QC, Canada
- 89 School of Physics, University of Melbourne, Victoria, Australia
- 90 Department of Physics, The University of Michigan, Ann Arbor, MI, United States
- 91 Department of Physics and Astronomy, Michigan State University, East Lansing, MI, United States
- 92 (a) INFN Sezione di Milano; (b) Dipartimento di Fisica, Università di Milano, Milano, Italy
- 93 B.I. Stepanov Institute of Physics, National Academy of Sciences of Belarus, Minsk, Belarus
- 94 National Scientific and Educational Centre for Particle and High Energy Physics, Minsk, Belarus
- 95 Group of Particle Physics, University of Montreal, Montreal, QC, Canada
- 96 P.N. Lebedev Physical Institute of the Russian Academy of Sciences, Moscow, Russia
- 97 Institute for Theoretical and Experimental Physics (ITEP), Moscow, Russia
- 98 National Research Nuclear University MEPhI, Moscow, Russia
- 99 D.V. Skobel'syn Institute of Nuclear Physics, M.V. Lomonosov Moscow State University, Moscow, Russia
- 100 Fakultät für Physik, Ludwig-Maximilians-Universität München, München, Germany
- 101 Max-Planck-Institut für Physik (Werner-Heisenberg-Institut), München, Germany
- 102 Nagasaki Institute of Applied Science, Nagasaki, Japan
- 103 Graduate School of Science and Kobayashi-Maskawa Institute, Nagoya University, Nagoya, Japan
- 104 (a) INFN Sezione di Napoli; (b) Dipartimento di Fisica, Università di Napoli, Napoli, Italy
- 105 Department of Physics and Astronomy, University of New Mexico, Albuquerque, NM, United States
- 106 Institute for Mathematics, Astrophysics and Particle Physics, Radboud University Nijmegen/Nikhef, Nijmegen, Netherlands
- 107 Nikhef National Institute for Subatomic Physics and University of Amsterdam, Amsterdam, Netherlands
- 108 Department of Physics, Northern Illinois University, DeKalb, IL, United States
- 109 Budker Institute of Nuclear Physics, SB RAS, Novosibirsk, Russia
- 110 Department of Physics, New York University, New York, NY, United States
- 111 Ohio State University, Columbus, OH, United States
- 112 Faculty of Science, Okayama University, Okayama, Japan
- 113 Homer L. Dodge Department of Physics and Astronomy, University of Oklahoma, Norman, OK, United States
- 114 Department of Physics, Oklahoma State University, Stillwater, OK, United States
- 115 Palacký University, RCPTM, Olomouc, Czech Republic
- 116 Center for High Energy Physics, University of Oregon, Eugene, OR, United States
- 117 LAL, Univ. Paris-Sud, CNRS/IN2P3, Université Paris-Saclay, Orsay, France
- 118 Graduate School of Science, Osaka University, Osaka, Japan
- 119 Department of Physics, University of Oslo, Oslo, Norway
- 120 Department of Physics, Oxford University, Oxford, United Kingdom
- 121 (a) INFN Sezione di Pavia; (b) Dipartimento di Fisica, Università di Pavia, Pavia, Italy
- 122 Department of Physics, University of Pennsylvania, Philadelphia, PA, United States
- 123 National Research Centre "Kurchatov Institute", B.P. Konstantinov Petersburg Nuclear Physics Institute, St. Petersburg, Russia
- 124 (a) INFN Sezione di Pisa; (b) Dipartimento di Fisica E. Fermi, Università di Pisa, Pisa, Italy

- ¹²⁵ Department of Physics and Astronomy, University of Pittsburgh, Pittsburgh, PA, United States
- ¹²⁶ ^(a) Laboratório de Instrumentação e Física Experimental de Partículas – LIP, Lisboa; ^(b) Faculdade de Ciências, Universidade de Lisboa, Lisboa; ^(c) Department of Physics, University of Coimbra, Coimbra; ^(d) Centro de Física Nuclear da Universidade de Lisboa, Lisboa; ^(e) Departamento de Física, Universidade do Minho, Braga; ^(f) Departamento de Física Teórica y del Cosmos and CAFPE, Universidad de Granada, Granada (Spain); ^(g) Dep Física and CEFITEC of Faculdade de Ciências e Tecnologia, Universidade Nova de Lisboa, Caparica, Portugal
- ¹²⁷ Institute of Physics, Academy of Sciences of the Czech Republic, Praha, Czech Republic
- ¹²⁸ Czech Technical University in Prague, Praha, Czech Republic
- ¹²⁹ Faculty of Mathematics and Physics, Charles University in Prague, Praha, Czech Republic
- ¹³⁰ State Research Center Institute for High Energy Physics (Protvino), NRC KI, Russia
- ¹³¹ Particle Physics Department, Rutherford Appleton Laboratory, Didcot, United Kingdom
- ¹³² ^(a) INFN Sezione di Roma; ^(b) Dipartimento di Fisica, Sapienza Università di Roma, Roma, Italy
- ¹³³ ^(a) INFN Sezione di Roma Tor Vergata; ^(b) Dipartimento di Fisica, Università di Roma Tor Vergata, Roma, Italy
- ¹³⁴ ^(a) INFN Sezione di Roma Tre; ^(b) Dipartimento di Matematica e Fisica, Università Roma Tre, Roma, Italy
- ¹³⁵ ^(a) Faculté des Sciences Ain Chock, Réseau Universitaire de Physique des Hautes Energies – Université Hassan II, Casablanca; ^(b) Centre National de l’Energie des Sciences Techniques Nucleaires, Rabat; ^(c) Faculté des Sciences Semlalia, Université Cadi Ayyad, LPHEA-Marrakech; ^(d) Faculté des Sciences, Université Mohamed Premier and LPTPM, Oujda; ^(e) Faculté des sciences, Université Mohammed V, Rabat, Morocco
- ¹³⁶ DSM/IRFU (Institut de Recherches sur les Lois Fondamentales de l’Univers), CEA Saclay (Commissariat à l’Energie Atomique et aux Energies Alternatives), Gif-sur-Yvette, France
- ¹³⁷ Santa Cruz Institute for Particle Physics, University of California Santa Cruz, Santa Cruz, CA, United States
- ¹³⁸ Department of Physics, University of Washington, Seattle, WA, United States
- ¹³⁹ Department of Physics and Astronomy, University of Sheffield, Sheffield, United Kingdom
- ¹⁴⁰ Department of Physics, Shinshu University, Nagano, Japan
- ¹⁴¹ Fachbereich Physik, Universität Siegen, Siegen, Germany
- ¹⁴² Department of Physics, Simon Fraser University, Burnaby, BC, Canada
- ¹⁴³ SLAC National Accelerator Laboratory, Stanford, CA, United States
- ¹⁴⁴ ^(a) Faculty of Mathematics, Physics & Informatics, Comenius University, Bratislava; ^(b) Department of Subnuclear Physics, Institute of Experimental Physics of the Slovak Academy of Sciences, Kosice, Slovak Republic
- ¹⁴⁵ ^(a) Department of Physics, University of Cape Town, Cape Town; ^(b) Department of Physics, University of Johannesburg, Johannesburg; ^(c) School of Physics, University of the Witwatersrand, Johannesburg, South Africa
- ¹⁴⁶ ^(a) Department of Physics, Stockholm University; ^(b) The Oskar Klein Centre, Stockholm, Sweden
- ¹⁴⁷ Physics Department, Royal Institute of Technology, Stockholm, Sweden
- ¹⁴⁸ Departments of Physics & Astronomy and Chemistry, Stony Brook University, Stony Brook, NY, United States
- ¹⁴⁹ Department of Physics and Astronomy, University of Sussex, Brighton, United Kingdom
- ¹⁵⁰ School of Physics, University of Sydney, Sydney, Australia
- ¹⁵¹ Institute of Physics, Academia Sinica, Taipei, Taiwan
- ¹⁵² Department of Physics, Technion: Israel Institute of Technology, Haifa, Israel
- ¹⁵³ Raymond and Beverly Sackler School of Physics and Astronomy, Tel Aviv University, Tel Aviv, Israel
- ¹⁵⁴ Department of Physics, Aristotle University of Thessaloniki, Thessaloniki, Greece
- ¹⁵⁵ International Center for Elementary Particle Physics and Department of Physics, The University of Tokyo, Tokyo, Japan
- ¹⁵⁶ Graduate School of Science and Technology, Tokyo Metropolitan University, Tokyo, Japan
- ¹⁵⁷ Department of Physics, Tokyo Institute of Technology, Tokyo, Japan
- ¹⁵⁸ Department of Physics, University of Toronto, Toronto, ON, Canada
- ¹⁵⁹ ^(a) TRIUMF, Vancouver, BC; ^(b) Department of Physics and Astronomy, York University, Toronto, ON, Canada
- ¹⁶⁰ Faculty of Pure and Applied Sciences, and Center for Integrated Research in Fundamental Science and Engineering, University of Tsukuba, Tsukuba, Japan
- ¹⁶¹ Department of Physics and Astronomy, Tufts University, Medford, MA, United States
- ¹⁶² Department of Physics and Astronomy, University of California Irvine, Irvine, CA, United States
- ¹⁶³ ^(a) INFN Gruppo Collegato di Udine, Sezione di Trieste, Udine; ^(b) ICTP, Trieste; ^(c) Dipartimento di Chimica, Fisica e Ambiente, Università di Udine, Udine, Italy
- ¹⁶⁴ Department of Physics and Astronomy, University of Uppsala, Uppsala, Sweden
- ¹⁶⁵ Department of Physics, University of Illinois, Urbana, IL, United States
- ¹⁶⁶ Instituto de Física Corpuscular (IFIC) and Departamento de Física Atomica, Molecular y Nuclear and Departamento de Ingeniería Electrónica and Instituto de Microelectrónica de Barcelona (IMB-CNM), University of Valencia and CSIC, Valencia, Spain
- ¹⁶⁷ Department of Physics, University of British Columbia, Vancouver, BC, Canada
- ¹⁶⁸ Department of Physics and Astronomy, University of Victoria, Victoria, BC, Canada
- ¹⁶⁹ Department of Physics, University of Warwick, Coventry, United Kingdom
- ¹⁷⁰ Waseda University, Tokyo, Japan
- ¹⁷¹ Department of Particle Physics, The Weizmann Institute of Science, Rehovot, Israel
- ¹⁷² Department of Physics, University of Wisconsin, Madison, WI, United States
- ¹⁷³ Fakultät für Physik und Astronomie, Julius-Maximilians-Universität, Würzburg, Germany
- ¹⁷⁴ Fakultät für Mathematik und Naturwissenschaften, Fachgruppe Physik, Bergische Universität Wuppertal, Wuppertal, Germany
- ¹⁷⁵ Department of Physics, Yale University, New Haven, CT, United States
- ¹⁷⁶ Yerevan Physics Institute, Yerevan, Armenia
- ¹⁷⁷ Centre de Calcul de l’Institut National de Physique Nucléaire et de Physique des Particules (IN2P3), Villeurbanne, France

^a Also at Department of Physics, King’s College London, London, United Kingdom.

^b Also at Institute of Physics, Azerbaijan Academy of Sciences, Baku, Azerbaijan.

^c Also at Novosibirsk State University, Novosibirsk, Russia.

^d Also at TRIUMF, Vancouver, BC, Canada.

^e Also at Department of Physics & Astronomy, University of Louisville, Louisville, KY, United States.

^f Also at Department of Physics, California State University, Fresno, CA, United States.

^g Also at Department of Physics, University of Fribourg, Fribourg, Switzerland.

^h Also at Departament de Física de la Universitat Autònoma de Barcelona, Barcelona, Spain.

ⁱ Also at Departamento de Física e Astronomia, Faculdade de Ciências, Universidade do Porto, Portugal.

^j Also at Tomsk State University, Tomsk, Russia.

^k Also at Università di Napoli Parthenope, Napoli, Italy.

^l Also at Institute of Particle Physics (IPP), Canada.

^m Also at National Institute of Physics and Nuclear Engineering, Bucharest, Romania.

ⁿ Also at Department of Physics, St. Petersburg State Polytechnical University, St. Petersburg, Russia.

^o Also at Department of Physics, The University of Michigan, Ann Arbor, MI, United States.

^p Also at Centre for High Performance Computing, CSIR Campus, Rosebank, Cape Town, South Africa.

- ^q Also at Louisiana Tech University, Ruston, LA, United States.
- ^r Also at Institutio Catalana de Recerca i Estudis Avancats, ICREA, Barcelona, Spain.
- ^s Also at Graduate School of Science, Osaka University, Osaka, Japan.
- ^t Also at Department of Physics, National Tsing Hua University, Taiwan.
- ^u Also at Institute for Mathematics, Astrophysics and Particle Physics, Radboud University Nijmegen/Nikhef, Nijmegen, Netherlands.
- ^v Also at Department of Physics, The University of Texas at Austin, Austin, TX, United States.
- ^w Also at CERN, Geneva, Switzerland.
- ^x Also at Georgian Technical University (GTU), Tbilisi, Georgia.
- ^y Also at Ochadai Academic Production, Ochanomizu University, Tokyo, Japan.
- ^z Also at Manhattan College, New York, NY, United States.
- ^{aa} Also at Hellenic Open University, Patras, Greece.
- ^{ab} Also at Academia Sinica Grid Computing, Institute of Physics, Academia Sinica, Taipei, Taiwan.
- ^{ac} Also at School of Physics, Shandong University, Shandong, China.
- ^{ad} Also at Moscow Institute of Physics and Technology State University, Dolgoprudny, Russia.
- ^{ae} Also at Section de Physique, Université de Genève, Geneva, Switzerland.
- ^{af} Also at Eotvos Lorand University, Budapest, Hungary.
- ^{ag} Also at Departments of Physics & Astronomy and Chemistry, Stony Brook University, Stony Brook, NY, United States.
- ^{ah} Also at International School for Advanced Studies (SISSA), Trieste, Italy.
- ^{ai} Also at Department of Physics and Astronomy, University of South Carolina, Columbia, SC, United States.
- ^{aj} Also at School of Physics and Engineering, Sun Yat-sen University, Guangzhou, China.
- ^{ak} Also at Institute for Nuclear Research and Nuclear Energy (INRNE) of the Bulgarian Academy of Sciences, Sofia, Bulgaria.
- ^{al} Also at Faculty of Physics, M.V. Lomonosov Moscow State University, Moscow, Russia.
- ^{am} Also at Institute of Physics, Academia Sinica, Taipei, Taiwan.
- ^{an} Also at National Research Nuclear University MEPhI, Moscow, Russia.
- ^{ao} Also at Department of Physics, Stanford University, Stanford, CA, United States.
- ^{ap} Also at Institute for Particle and Nuclear Physics, Wigner Research Centre for Physics, Budapest, Hungary.
- ^{aq} Also at Flensburg University of Applied Sciences, Flensburg, Germany.
- ^{ar} Also at University of Malaya, Department of Physics, Kuala Lumpur, Malaysia.
- ^{as} Also at CPPM, Aix-Marseille Université and CNRS/IN2P3, Marseille, France.
- ^{at} Also affiliated with PKU-CHEP.
- * Deceased.